

Old Carbon, New Insights: Thermal Reactivity and Bioavailability of Saltmarsh Soils

Alex Houston¹, Mark H Garnett², ~~Jo Smith³~~, and William E N Austin^{1,3,4}

1. Department of Geography and Sustainable Development, University of St Andrews, St Andrews, KY16 9AL, United Kingdom
2. NEIF Radiocarbon Laboratory, Scottish Universities Environmental Research Centre, East Kilbride, G75 0QF, United Kingdom
- ~~3. Institute of Biological & Environmental Sciences, School of Biological Science, University of Aberdeen, Aberdeen, AB24 3FX, United Kingdom~~
- ~~4.3.~~ Scottish Association of Marine Science, Oban, PA37 1QA, United Kingdom

Correspondence to: Alex Houston (ah383@st-andrews.ac.uk)

Abstract

Saltmarshes are globally important coastal wetlands which can ~~help store carbon for millennia, helping~~ to mitigate the impacts of climate change. They accumulate organic carbon from both ~~modern and aged autochthonous~~ sources ~~through in-situ biological (above- and belowground plant production)~~ and ~~the capture of ex-situ autochthonous~~ sources ~~which are (terrestrial and marine sediments)~~ deposited during tidal inundation. Previous studies have found that long-term organic carbon storage in saltmarsh soils is driven by the ~~net contribution from the older pre-aged autochthonous~~ fraction, implying that ~~the inputs of young autochthonous~~ organic carbon ~~derived from in situ production are~~ recycled at a faster rate. However, ~~it is also acknowledged that the bioavailability of soil organic carbon depends as much upon environmental conditions as the reactivity of the organic carbon itself. Until now, there has been no empirical evidence linking the reactivity of saltmarsh soil organic carbon with its bioavailability for remineralization.~~

~~Using~~ We found that the ¹⁴C age of CO₂ produced during ramped oxidation, ~~we assessed the composition (¹⁴C and ¹³C) of saltmarsh soil carbon pools defined by their thermal reactivity. By relating ¹⁴C measurements of the soil carbon pools to CO₂ respired in aerobic incubations of soils from the same soils, we provide the first empirical evidence linking the thermal reactivity of saltmarsh soil organic carbon with its bioavailability for remineralization.~~

~~We found that old (¹⁴C saltmarsh ranged from 201 to 14,875 years BP, and that ¹⁴C-depleted) (older) carbon evolved from higher temperature ramped oxidation fractions, indicating that older carbon~~

Formatted: Plain Table 5

Formatted: Font: +Body (Aptos), Font color: Auto

Formatted: Heading 1, Line spacing: single

Formatted: Font: +Body (Aptos), 11 pt, Font color: Auto

Formatted: Heading 2, Line spacing: single

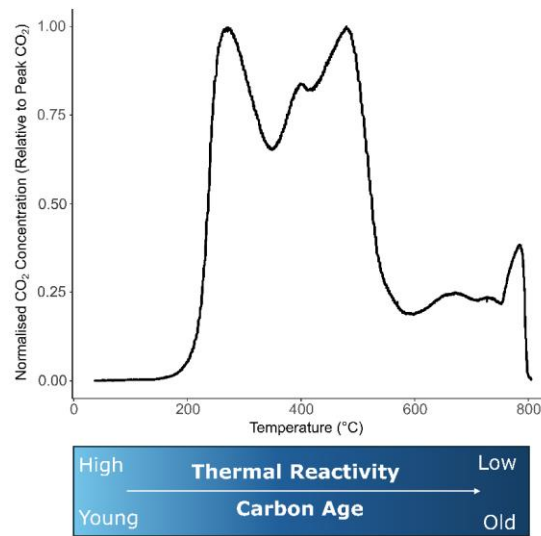
Formatted: Header

Formatted: Plain Table 5

dominates the thermally recalcitrant ~~organic carbon pools, whereas the thermally labile carbon is composed of younger organic carbon sources.fractions~~. In most cases, the ^{14}C content of the ~~lowest temperature ramped oxidation fraction (the most thermally labile carbon poolorganic C source)~~ was closest to the previously reported ^{14}C content of the CO_2 evolved from aerobic incubations of the same soils, implying that the ~~tatter was from a thermally labile organic carbon source. This implies that the~~ bioavailability of saltmarsh soil organic carbon to remineralisation in oxic conditions is closely related to its thermal lability.

Our results highlight the importance of saltmarshes as stores of both old, thermally recalcitrant organic carbon, as well as younger, thermally labile organic carbon that is vulnerable to decomposition under oxic conditions.reactivity. Management interventions (e.g. rewetting by tidal inundation) to limit the exposure of saltmarsh soils to elevated oxygen availability may help to protect and conserve these stores of ~~thermallyold~~, labile organic carbon and hence limit CO_2 emissions. We also present the first evidence to support the inclusion of thermally labile allochthonous OC stored in saltmarsh soils in additionality assessments, with relevance to international carbon crediting projects and National GHG Inventories.

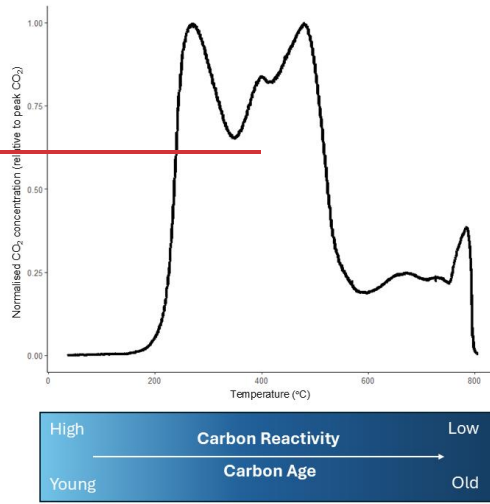
Graphical Abstract



Formatted: Font: +Body (Aptos), 11 pt, Font color: Auto

Formatted: Heading 2, Justified, Line spacing: single

Formatted: Header



1. Introduction

Saltmarshes accumulate organic carbon (OC) of variable age and reactivity into their soils. A portion of this OC is stored for millennia, providing a climate regulation service, and some is returned to the atmosphere or laterally exported (Komada et al., 2022; Macreadie et al., 2021). Saltmarshes also accumulate and produce inorganic carbon (IC) but the climate regulation service of this is currently under debate and unclear (Granse et al., 2024; Van Dam et al., 2021).

To understand the role of saltmarsh soils in carbon cycling and their potential for climate mitigation through targeted management interventions, much research has focussed on determining the autochthonous (in-situ) and allochthonous (ex-situ, trapped during tidal inundation from terrestrial and marine sources) contributions to saltmarsh soils, with the accumulation of autochthonous OC as a direct sequestration of carbon from the atmosphere, reducing the amount of atmospheric greenhouse gases (GHGs) (Macreadie et al., 2019; Saintilan et al., 2013; Van de Broek et al., 2018). The accumulation of allochthonous OC, originally sequestered outside the saltmarsh area, does not directly reduce atmospheric GHGs, but can represent a source of avoided emissions if it remains stored in the saltmarsh soil for longer than in an alternative depositional environment (Howard et al., 2023). Evidence to determine whether this is the case or not, and under what scenarios, has proven challenging to obtain (Gerald et al., 2019; Houston et al., 2024a). OC pools with distinct biological turnover times may instead provide greater insights(Houston et al., 2024).

Another approach is to partition the saltmarsh soil OC pool by reactivity (Luk et al., 2021), which may provide greater insight into the soil carbon residence time and therefore the climate mitigation achieved through targeted management interventions to retain that carbon (Sanderman and Grandy, 2020). Soil OC reactivity can be defined as its availability for remineralisation by soil microbial communities, with different reactivity pools having different turnover times (Plante et al., 2009).

Ramped oxidation (RO) and ramped pyrolysis oxidation (RPO) have been used to estimate the thermal reactivity and biological turnover time of soil and sediment OC (Hemingway et al., 2017b; Plante et al., 2011; Rosenheim et al., 2008). RO and RPO involve measuring the quantity of CO₂ evolved as a sample is increasingly heated at a constant rate in an atmosphere containing oxygen (e.g., Plante et al., 2011; Stoner et al., 2023), or other gases, typically Helium (RPO: e.g., Hemingway et al., 2017a; Rosenheim et al., 2008). The temperature at which CO₂ is thermally-evolved is related to the activation energy required to thermally decompose C (Hemingway et al., 2017b), which is also an estimate of the energy required for biological degradation of OC (Peltre et al., 2013; Plante et al., 2013). CO₂ evolved at low temperatures is deemed to be from soil OC pools with a greater thermal lability than CO₂ evolved at higher temperatures (Peltre et al., 2013; Rosenheim et al., 2008). OC thermal reactivity pools can be examined by collecting the evolved CO₂ from set temperature ranges with distinct thermal reactivities and measuring the ¹⁴C (age) and ¹³C content (Rosenheim et al., 2008), which can then be related to the activation energy required to thermally decompose those C sources (Hemingway et al., 2017b).

The ¹⁴C content of the thermal reactivity pools provides insight into the turnover time of each pool, with past research showing that the oldest soil organic matter (OM) (most depleted ¹⁴C content) tends to dominate the most thermally recalcitrant fractions (Bao et al., 2019b; Plante et al., 2013; Stoner et al., 2023). Similar results have been found for saltmarsh soils (Luk et al., 2021). Young OC, which can be autochthonous or allochthonous (Van de Broek et al., 2018), has been found to turnover at a faster rate than old OC in saltmarsh soils (Komada et al., 2022; Van de Broek et al., 2018), implying that young OC may tend to be more thermally labile than old OC for saltmarsh soils.

The ¹³C content of the thermal reactivity pools can also provide insight as to whether the source of OC has an influence on turnover time. Previous work has found that the ¹³C content of evolved CO₂ tends to be more enriched at higher temperatures due to greater contributions from ¹³C-enriched, degraded/microbially derived OC (Luk et al., 2021; Sanderman and Grandy, 2020; Stoner et al., 2023). Similarly, comparisons of the isotopic composition of thermally-defined OC

pools to their chemical properties have found that thermally labile OC is derived from mostly lipids and polysaccharides, whereas OC with a higher thermal recalcitrance is derived from a greater proportion of phenolic and aromatic compounds (Sanderman and Grandy, 2020). The thermal reactivity of soil and sediment OC is also influenced by the formation of organo-mineral complexes, which can physically and chemically stabilise OC (Bianchi et al., 2024; Hemingway et al., 2019). Mineral-associations can increase the energy required for decomposition and have been found to increase thermal recalcitrance and to slow turnover times of soil and sediment OC (Hemingway et al., 2019; Stoner et al., 2023).

Crucially, the biological availability (bioavailability) of OC for decomposition, and hence its biological turnover time, depends on the prevailing environmental conditions as well as thermal reactivity (Hemingway et al., 2017b; Schmidt et al., 2011). For example, increased hydrodynamic energy can destabilise organo-mineral complexes and increase the bioavailability of previously stable OC (Spivak et al., 2019). Similarly, increased oxygen availability can decrease the energy requirement for microbes to decompose molecularly recalcitrant OC, causing it to be remineralised at a faster rate (Noyce et al., 2023).

Houston et al. (2024b) found that young OC stored in saltmarsh soils was preferentially respired as carbon dioxide (CO₂) during aerobic incubation experiments, but that a portion of the respired CO₂ was produced from an aged (¹⁴C-depleted), allochthonous source. It is possible that this CO₂ could have been respired from thermally labile as well as thermally recalcitrant soil OC sources because the increased oxygen availability of the incubations potentially facilitated the degradation of OC which was previously stable in the low-oxygen environment of typical saltmarsh soils (Noyce et al., 2023).

The isotopic composition of RO thermal reactivity fractions can be compared to the isotopic composition of the CO₂ that is evolved biologically during incubations of equivalent samples to determine whether or not the age of the most biologically- and thermally-reactive OC pools match. Here, we present the first measurements of the ¹³C and ¹⁴C content of CO₂ derived from saltmarsh soils using RO, and the first comparison of these to the ¹⁴C content of biologically evolved CO₂ from the same soils (Houston et al., 2024b). We hypothesised that the thermally labile C pools would be composed of younger C than the thermally recalcitrant pools, and that the CO₂ evolved from saltmarsh soils exposed to oxic conditions (Houston et al., 2024b) are from a predominantly thermally labile OC pool.

The proportions of autochthonous and allochthonous OC accumulating in saltmarsh soils and OC reactivity pools are thought to be related, as in-situ processes during burial of saltmarsh soils

have been suggested to favour the long-term storage of aged, allochthonous OC (Komada et al., 2022; Leorri et al., 2018; Mueller et al., 2019; Van de Broek et al., 2018). Young OC, which can be autochthonous or allochthonous (Van de Broek et al., 2018), is hypothesised to turnover at a faster rate, often resulting in its remineralisation to the atmosphere. It is therefore assumed that old OC is mostly composed of recalcitrant (low reactivity) components, whereas young OC contains a greater proportion of labile (reactive) components (Komada et al., 2022; Van de Broek et al., 2018). Of course, this is not always the case as young OC can contain recalcitrant material, and older OC can be labile if it was stored in a stable environment with low carbon turnover rates, such as a permafrost soil, prior to its mobilisation (Dasari et al., 2024).

Houston et al. (2024) found that a portion of the carbon dioxide (CO_2) evolved during aerobic incubations of saltmarsh soils was from an old, allochthonous source. It is possible that the CO_2 could have been evolved from a labile source, or a physically stabilized source that decomposed due to increased oxygen availability (a thermodynamically favourable terminal electron acceptor facilitating the degradation of OC which was stable in a low-oxygen environment, as saltmarsh soils typically are (Noyce et al., 2023)). To constrain these sources, the ^{14}C composition of the biologically evolved CO_2 from these experiments can be directly compared to the ^{14}C composition of the thermally characterized soil OC.

The thermal reactivity of soil OC can usefully be approximated using ramped oxidation (RO), which involves measuring the quantity of CO_2 evolved as a sample is increasingly heated at a constant rate in an atmosphere containing oxygen (Garnett et al., 2023). The energy required to thermally evolve CO_2 is expected to be related to the energy required for biological degradation of OC, with CO_2 evolved at low temperatures deemed to be from more reactive soil OC pools than CO_2 evolved at higher temperatures (Peltre et al., 2013). The age of the OC reactivity pools can be examined by collecting the evolved CO_2 from set temperature ranges and measuring the ^{14}C (age) content (Garnett et al., 2023; Plante et al., 2013). These can be compared to the ^{14}C content of the CO_2 that is evolved biologically during incubations of equivalent samples to determine whether the age of the most biologically and thermally reactive OC pools match, or not (Plante et al., 2011).

The ^{14}C content of the thermal reactivity pools also provides insight into the turnover time of each pool, with past research showing that the oldest soil organic matter (OM) (most depleted ^{14}C content) tends to dominate the most thermally stable fractions (Bao et al., 2019; Plante et al., 2013; Stoner et al., 2023). Similar results have been found for saltmarsh soils (Luk et al., 2021). The ^{13}C content of the thermal reactivity pools can also provide insight as to whether the source

of OC has an influence on turnover time. Previous work shows that the ^{13}C content of evolved CO_2 tends to be more enriched at higher temperatures due to greater contributions from ^{13}C -enriched, degraded/microbially derived C (Luk et al., 2021; Sanderman and Grandy, 2020; Stoner et al., 2023). Here, we present the first measurements of the ^{13}C and ^{14}C content of CO_2 derived from saltmarsh soils using ramped oxidation, and the first comparison of these to the ^{14}C content of biologically evolved CO_2 from the same soils (Houston et al., 2024). We hypothesised that the pre-aged, allochthonous CO_2 respired from saltmarsh soils in Houston et al. (2024) was from a thermally labile source, and that the thermally recalcitrant OC pools would be predominantly composed of older OC.

Formatted: Plain Table 5

2. Methods

Formatted: Justified

2.1. Field site and sample collection

Three saltmarsh soil cores (T1-3) were retrieved ca. 30 m apart from the lower marsh zone from Skinflats (SK), an estuarine saltmarsh in Scotland (56° 3'34.04"N, 3°43'59.16"W), as detailed in Houston et al. (2024b2024). Field methods and laboratory sub-sampling procedures are described in detail in Houston et al. (2024b2024). Briefly, the cores were split into 1 cm thick slices as follows: core T1 (0-1 cm, 5-6 cm, and 18-19 cm); T2 (0-1 cm, 5-6 cm, and 15-16 cm), and T3 (0-1 cm, 5-6 cm, and 19-20 cm) (with the deepest sample from each core being the deepest retrieved sample from the 20 cm length of the corer. On the occasions when a full core was not retrieved, the deepest retrieved soil was used). Each slice was subsequently divided to provide sample material for the RO procedure, and for aerobic laboratory incubations from which the biologically evolved CO_2 was collected for ^{13}C and ^{14}C analysis (Houston et al., 2024b2024).

Field Code Changed

2.2. Ramped oxidation

The RO sub-samples were individually dried to constant mass before milling to a fine powder to homogenise and limit potential shielding effects from aggregates. Unlike most RO and RPO studies (e.g., Hemingway et al., 2017b), we did not remove carbonates from our samples. Acid treatment, which is required to remove carbonates from samples has been demonstrated to result in losses from the labile OC fraction (Bao et al., 2019a). A loss of labile OC for our samples could seriously impact the interpretations in our study, and our ability to compare the ^{14}C content of the CO_2 respired from bulk (untreated) soils in the incubation experiments (Houston et al., 2024b) to the ^{14}C content of the RO thermal fractions.

Formatted: Header

Formatted: Plain Table 5

The samples were then sent to the NEIF Radiocarbon Laboratory for the RO procedure, which is described in Garnett et al. (2023). The RO procedure involved two stages, a first combustion to determine the relationship between the rate of CO₂ evolution and temperature (thermogram), and a second combustion where evolved sample gases were collected across defined temperature ranges, for subsequent isotope analysis. For the first combustion, ca. 200 mg of dried and homogenized sample material was weighed into a quartz vial which was inset into a quartz combustion tube, which was subsequently placed into a furnace set initially to room temperature. The furnace was (2023). In brief, the samples were progressively heated at a constant rate of 5°C per minute from ambient room temperature to 800°C in a stream of high purity oxygen (N5.5, BOC, UK). Heating caused combustion of the sample and the evolution of gas which was passed into a second quartz combustion tube containing platinised wool in a furnace set to a constant temperature of 950°C. The platinised wool acted as a catalyst to ensure complete combustion of the evolved gases. Upon exiting the secondary combustion chamber the sample passed through a glass tube containing magnesium perchlorate desiccant to remove moisture and subsequently the CO₂ concentration of the gas was and the evolved CO₂ measured using a non-dispersive infrared CO₂ sensor (SprintIR®-WF-5, Gas Sensing Solutions, UK). The sample was then passed out of the sensor unit and vented to the atmosphere.

The measured CO₂ concentration (normalised for sample mass) was plotted against temperature to produce thermograms which were used to identify temperature ranges, which defined C thermal. Temperature ranges, which defined OG reactivity pools for this study, were identified from the resulting thermograms: 150-325 °C, (t1), 325-425 °C, (t2), 425-500 °C, (t3), 500-650 °C, (t4), and 650-800 °C.

For each sample, the required mass of material to evolve sufficient CO₂ (> 3 mL) for ¹⁴C measurement was calculated based on the thermogram. A new sub-set from the original dried and homogenised sample (t5). The RO procedure was then re-run following the RO procedure outlined above, but instead of venting to atmosphere, after its measurement the evolved CO₂ was collected into foil gas bags based on the defined temperature ranges. CO₂ was with new sample material and the thermally evolved CO₂ collected for ¹³C analysis from 650-800 °C, but sufficient CO₂ was evolved for ¹⁴C analysis from this thermal fraction for only one sample (T1 0.5 cm, Table A1) and we do not consider this fraction further because it is likely dominated by carbonates and not relevant to the purpose of this study.

The foil gas bags (5 L Spout Pouch, <https://www.pouchshop.co.uk/>) used for sample collection were sealed with one-hole rubber bungs into which a 0.6 cm diameter x 5 cm length stainless

Formatted: Header

steel tube was inserted. Isoversinic tubing (Saint Gobain, France) was fitted over the stainless steel to connect it to a quick coupling (Colder Products Company, USA), which allowed connection to the RO kit.

Prior to the RO CO₂ collection, all equipment was cleaned using a standardised procedure (Garnett et al., 2023). All glassware was combusted at 900°C for a minimum of two hours, and all couplings and connectors were washed in carbon-free detergent (Decon) and rinsed in Milli-Q water. The foil gas bags were cleaned by repeatedly (3 times) filling with ca. 1 L high purity nitrogen gas (Research Grade 99.9995% purity, BOC, UK) and evacuating with an air pump, over a period of at least 24 hours (to aid out-gassing of CO₂). The final evacuation, immediately before connecting to the RO rig, involved pumping out the bags with an SBA-5 CO₂ analyser (PPsystems, USA) to ensure that the bags did not contain significant contamination. Before commencing a sample combustion, the entire RO rig was checked for leaks and other potential sources of contamination by measuring the CO₂ concentration in the oxygen carrier gas exiting the kit, using the SBA-5 CO₂ analyser.

Within 3 days of combusting a sample, the evolved gas in each foil bag was connected to a vacuum rig for and ¹⁴C analyses from the pre-defined temperature increments. The ¹³C and ¹⁴C analyses of these CO₂ samples followed the same methodology at the same laboratory as in Houston et al. (2024). Briefly, following cryogenic recovery of pure sample CO₂ by passing it through slush (-78°C; dry ice and industrial methylated spirits) and then liquid nitrogen (-196°C) traps, under high vacuum (ca. 3 x 10⁻³ millibars). The sample CO₂ was then split into three aliquots: One for δ¹³C analysis using isotope ratio mass spectrometry (IRMS; Delta V, Thermo-Fisher, Germany), one for graphitisation and subsequent AMS ¹⁴C analysis, and one for an archive back-up. The purification, the recovered sample CO₂ was graphitised AMS samples were measured and analysed for ¹⁴C content at the SUERC AMS Scottish Universities Environmental Research Centre Accelerator Mass Spectrometry (AMS) Laboratory (see Ascough et al., 2024). The ¹³C. A sub-sample of the recovered CO₂ was analysed for ¹³C content (δ¹³C-VPDB) was using isotope ratio mass spectrometry (Thermo-Fisher Delta V, Germany) and used to normalise the ¹⁴C results to a δ¹³C of -25 ‰ to correct for isotopic fractionation. Following convention, ¹⁴C results are presented as %Modern (fraction modern x 100) and conventional radiocarbon ages (years BP, where 0 BP = AD 1950 and age = -8033 x Ln (%Modern/100)).

2.3. Data Analysis

Continuous activation energy distributions were modelled from thermograms using the 'rampedpyrox' package in Python V3.8 (Hemingway, 2016; Hemingway et al., 2017b). The

Formatted: Plain Table 5

rampedpyrox model calculates mean activation energies (μE) and the standard deviation of activation energy (σE), which is a measure of the heterogeneity of bond strength, for each temperature fraction which CO_2 was collected from. Mean μE , σE and activation energy distribution ($p(\sigma, E)$) are also calculated for each sample using the *rampedpyrox* model. We do not use the *rampedpyrox* model for calculation of isotope values as it applies a blank correction to ^{14}C (Hemingway et al., 2017a, b) which is not relevant to the analytical set-up for this study (Garnett et al., 2023), and the ^{13}C values generated varied significantly from our IRMS measured values (Table A2). Further data analysis and visualisation of thermograms and isotopic data was undertaken using RStudio V4.2.2 (R Core Team, 2022).

3. Results

Formatted: Justified

3.1. Radiocarbon

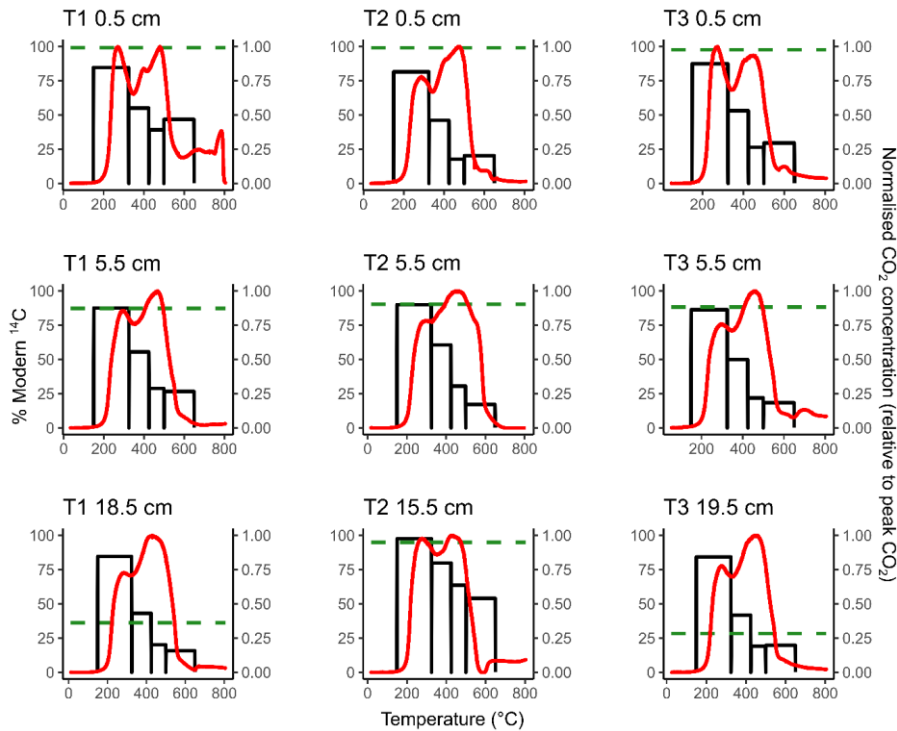


Figure 1. Thermograms

Formatted: Font: 11 pt

The CO_2 evolved from the RO analysis had bimodal distributions for most samples, with the major peaks occurring at approximately 250°C and 450°C (Fig. 1). These peaks were within t1 (150-

Formatted: Font: +Headings (Aptos Display), Not Bold, Font color: Accent 1

Formatted: Header

Formatted: Plain Table 5

325°C) and t3 (425-500°C), respectively. We calculated the proportion of CO₂ evolved from the lower temperature CO₂ peak (150-425°C; t1 and t2 combined) and the proportion of CO₂ evolved from the higher temperature CO₂ peak (425-650°C; t3 and t4 combined) (Table A1). There were no significant trends with depth for either T1, T2, or T3 (spearman's rho, p > 0.05). Visually, for both T1 and T3 the size of the second major peak relative to the lower temperature peak increased with depth, whereas for T2 the opposite was the case (Fig. 1). Most of the samples showed similar trends for CO₂ produced during the ramped combustion procedure, with a lesser CO₂ peak (t2, 325-425°C) between the two larger peaks of t1 and t3 (Fig. 1; see graphical abstract for magnified example). Following the t3 peak (425-500°C) there was another smaller peak in CO₂ evolution between 500-650°C (t4) (Fig. 1). T1 0.5 cm and T3 5.5 cm had high temperature CO₂ peaks between 650-800°C, but this peak was not present for most of the samples (Fig. 1).

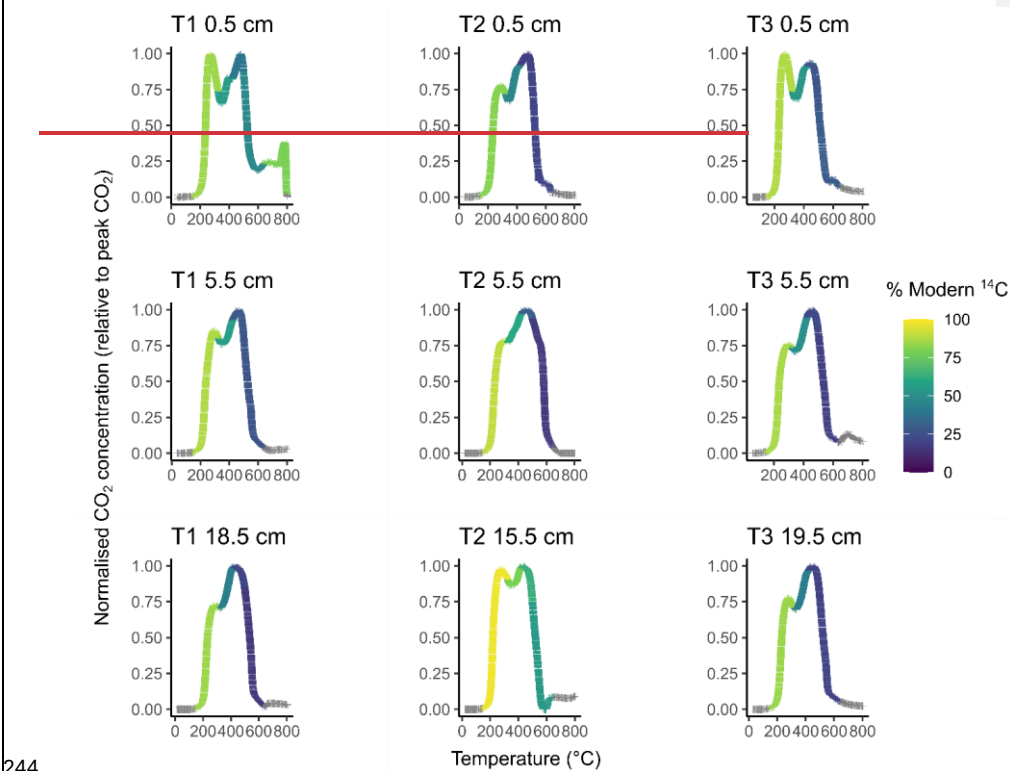


Figure 1. (red lines, right-hand y-axis) overlaying the Thermograms for each of the soil samples. The shading colour indicates the % Modern ¹⁴C content of the CO₂ evolved throughout the ramped oxidation from

Formatted: Font: 11 pt

Formatted: Font: 11 pt

Formatted: Font: 11 pt

Formatted: Header

temperature fractions (black bars, left-hand y-axis) for each sample. The horizontal green dashed lines represent the 150-325°C, 325-425°C, 425-500°C, 500-650°C (and 650-800°C for T1 0.5 cm only). Grey shading indicates values outside of the CO₂ collection range (150-800°C).

~~3.2. ¹⁴C content of the CO₂ respired from the aerobic incubation experiments of Houston et al. (2024b). ramped oxidation fractions.~~

The ¹⁴C content of the CO₂ evolved during the ramped oxidation (¹⁴C-RO fractions) decreased exponentially from 150-650°C (t1-t4) (p<0.001, Fig. 12, Table 1) were statistically similar between the 0.5 cm, 5.5 cm, and deepest sample (T1 18.5 cm, T2 15.5 cm, T3 19.5 cm) depth increments for). This regression was calculated using the mid-point of each of the temperature fractions (Kruskal-Wallis: p = 0.83, 0.38, 0.66, 0.99, for 150-325°C, 325- 425°C, 425-500°C, 500-650°C, respectively). There were, however, clear differences range (e.g., t1 mid-point is 237.5°C). Sufficient CO₂ for ¹⁴C analysis for 650-800°C (t5) was only recovered from one sample (T1 0.5 cm; Fig. 1, Table 1). This sample did not follow the same decreasing trend in ¹⁴C contents between the content with increasing temperature fractions, with ranges, as it contained a greater amount of 81.50-97.54 ‰ (79.75 ± 0.37 ‰ Modern for 150-325 °C, 41.67-79.80 ‰) than t2, t3 and t4 (39.18–55.02 ‰ Modern for 325-425 °C, 17.67-63.56 ‰ Modern for 425-500 °C, and 15.69-53.96 ‰ Modern for 500-650 °C (Fig. 1, Table 1).

)(Fig. 1, Table 1).

Formatted: Plain Table 5

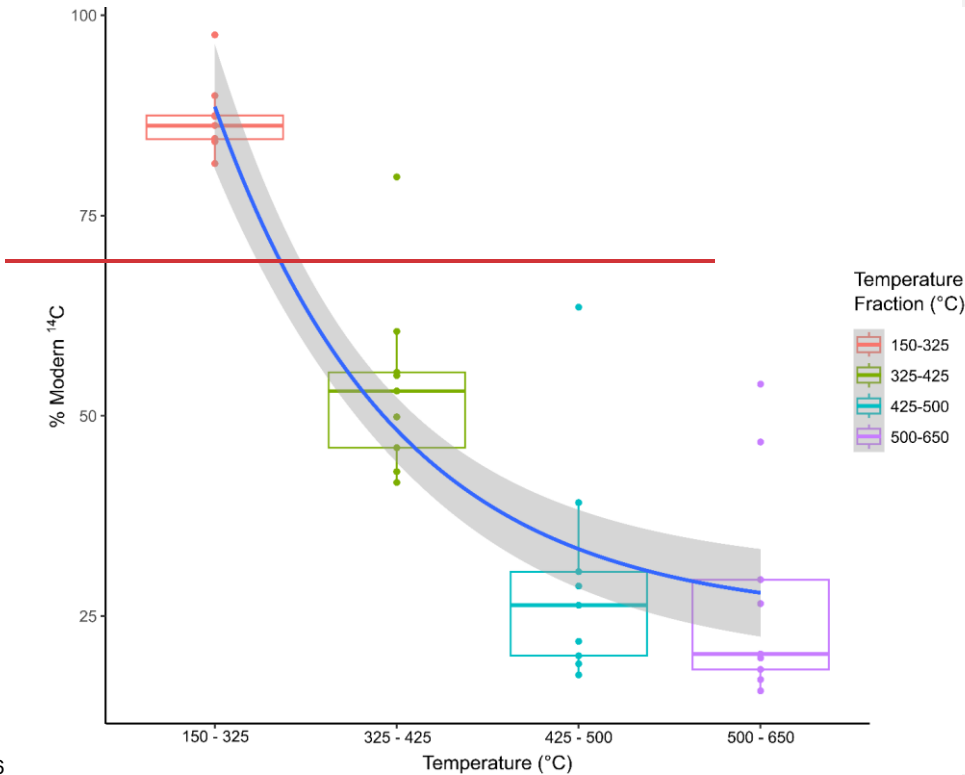
Formatted: Font: 11 pt

Formatted: Font: Not Bold, Font color: Text 2

Formatted: Caption, Justified

Formatted: Font: 9 pt, Not Bold

Formatted: Header



Formatted: Plain Table 5

Figure 2. Radiocarbon concentration (% Modern) of RO the CO_2 evolved from each temperature window during RO (150-325°C, 325-425°C, 425-500°C, 500-650°C). The blue line is the exponential regression between temperature and ^{14}C content ($y = 215.76e^{-0.004x}$, $p < 0.001$, $R^2 = 0.77$, $SE = 1.86$, $n = 36$). The grey shading is the 95% confidence interval of the regression.

Formatted: Font: 11 pt

Formatted: Font: 11 pt

For the entire sample set, the ^{14}C content of the evolved CO_2 ranged from 97.53 ± 0.50 % Modern for T2 15.5 cm (201 ± 41 years BP) to 15.70 ± 0.12 % Modern for T1 18.5 cm ($14,875 \pm 61$ years BP) (Fig. 2, Table 1, Table A2). There were no significant trends in ^{14}C content with depth, for example the ^{14}C contents of the CO_2 evolved from the 150-325°C fraction for the deepest layer (T1 18.5 cm, T2 15.5 cm, T3 19.5 cm), ranged from 84-97 % Modern (1,347-201 years BP), whereas in the surface (0.5 cm) samples it ranged from 81-87 % Modern (1,643-1,085 years BP) (Table 1, Table A2). The CO_2 evolved from the 500-650°C fraction for the deepest layer (T1 18.5 cm, T2 15.5 cm, T3 19.5 cm), ranged from 15-54 % Modern (14,875-4,956 years BP), whereas in the surface (0.5 cm) samples it ranged from 20-47 % Modern (12,826-6,108 years BP) (Table 1, Table A2).

Formatted: Font: Aptos, Font color: Black, Ligatures: None

Formatted: Line spacing: single

Formatted: Font: 11 pt

Formatted: Header

Table 1. fractions and the CO_2 produced in soil Radiocarbon concentration (% Modern) of the CO_2 evolved from each RO temperature fraction and the incubation experiments in Houston et al. (2024b). Errors are

282 reported to one standard deviation from the mean. A sole ¹⁴C measurement for T1 0.5 cm 650-
283 800 °C is reported in Table A1. (2024).

	% Modern ¹⁴ C				
	150-325°C	325-425°C	425-500°C	500-650°C	650-800°C
T1 0.5 cm	84.62 ± 0.44	55.02 ± 0.29	39.18 ± 0.21	46.75 ± 0.26	79.75 ± 0.37
T1 5.5 cm	87.51 ± 0.43	55.43 ± 0.28	28.76 ± 0.17	26.56 ± 0.16	
T1 18.5 cm	84.56 ± 0.44	43.06 ± 0.23	20.07 ± 0.13	15.70 ± 0.12	
T2 0.5 cm	81.50 ± 0.43	46.04 ± 0.24	17.67 ± 0.13	20.26 ± 0.14	
T2 5.5 cm	89.95 ± 0.42	60.55 ± 0.30	30.54 ± 0.17	17.11 ± 0.12	
T2 15.5 cm	97.53 ± 0.50	79.80 ± 0.41	63.56 ± 0.31	53.96 ± 0.27	
T3 0.5 cm	87.37 ± 0.45	53.09 ± 0.28	26.37 ± 0.15	29.55 ± 0.17	
T3 5.5 cm	86.23 ± 0.42	49.86 ± 0.25	21.87 ± 0.14	18.36 ± 0.12	
T3 19.5 cm	84.23 ± 0.41	41.67 ± 0.22	19.04 ± 0.13	19.76 ± 0.14	

284
285 3.2. ^{δ13}C

286 There were no significant differences in the ¹³C content of the
287 ramped oxidation fractions (Fig. 2, Table 2)

288 There was a positive linear relationship between the depth increments (Kruskal-Wallis; p = 0.66,
289 0.63, 0.63, 0.44, 0.17, ¹³C content of the evolved CO₂ (¹³C-RO) and temperature from the RO
290 analysis between 150-650°C (p<0.001, Fig. 3). As for Fig. 2, this regression was calculated using
291 the mid-point of each temperature range (e.g., t1 mid-point is 297.5°C).

Formatted: Plain Table 5

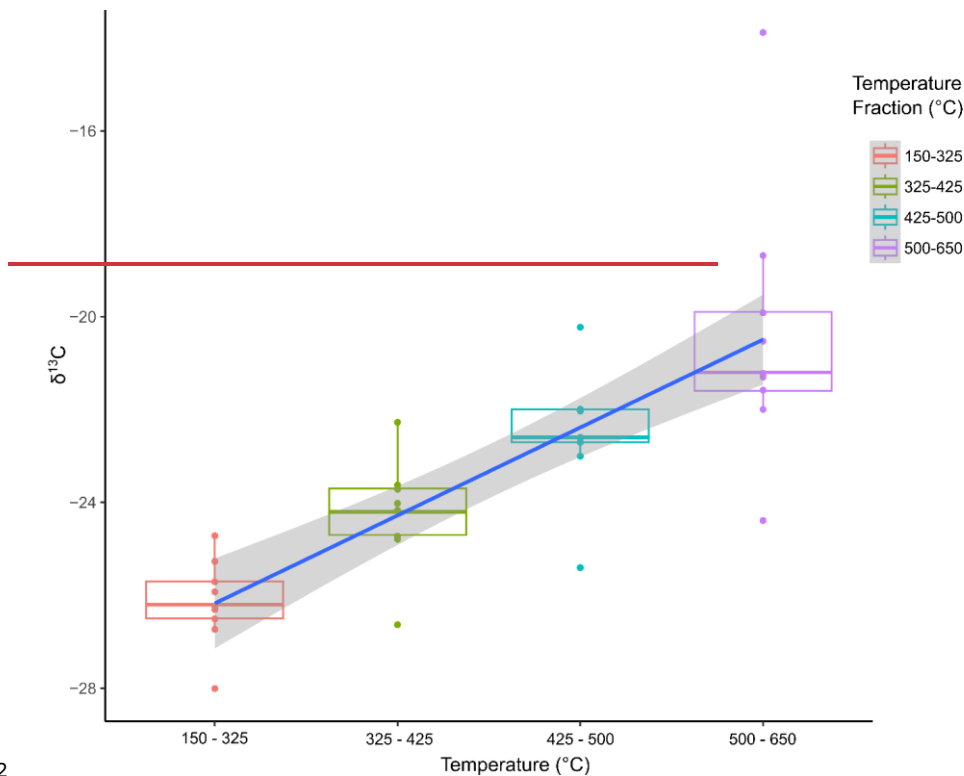


Figure 3. $\delta^{13}\text{C}$ content of the CO_2 evolved from each temperature window during RO (150-325 °C, 325-400 °C, 425-500 °C, 500-650 °C, 650-800 °C respectively). $\delta^{13}\text{C}$ contents followed the opposite trend to $\delta^{14}\text{C}$ contents with temperature, with ranges of ‰. The blue line is the linear regression between temperature and $\delta^{13}\text{C}$ content ($y = 0.017x - 30.39$, $p < 0.001$, $R^2 = 0.62$, $SE = 1.72$, $n = 45$). The grey shading is the 95 % confidence interval of the regression.

$\delta^{13}\text{C}$ values of the RO temperature fractions ranged from -28.0 ‰ to -24.7 ‰ (Table 2). Values for 150-325 °C, -26.6 to -22.3 ‰ (t1-t4), the range at which $\delta^{14}\text{C}$ was also measured (except for 325-425 one $\delta^{14}\text{C}$ measurement from the 650-800 °C, -25.4 to -20.2 ‰ fraction for 425-500 °C, -24.4 to -20.5 ‰) ranged from -28.0 ‰ to -13.9 ‰ for 500-650 °C (Fig. 3, Table 2), and -21.1 to -4.0 ‰ values for 650-800 °C (Fig. 2, Table 2).

Formatted: Header

Formatted: Plain Table 5

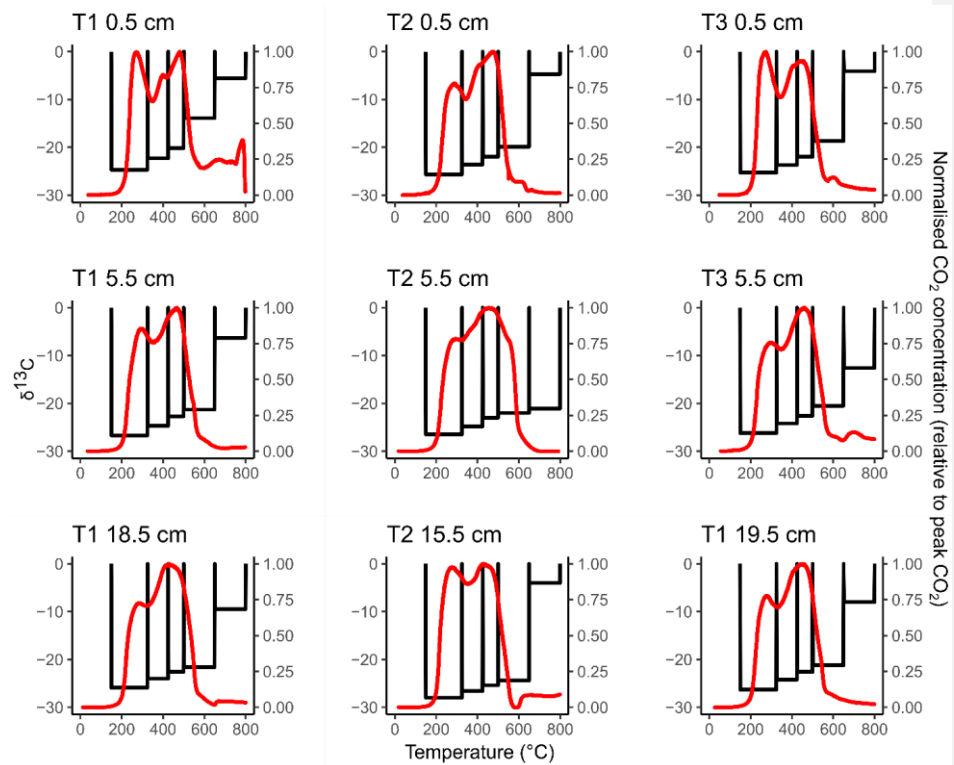


Figure 2. Thermograms (red lines, right-hand y-axis) overlaying the ^{13}C content of the RO temperature fractions (black bars, left-hand y-axis) for each sample. Unlike Fig. fraction (t5) ranged from -21.1, we did not attempt to relate the ^{13}C -RO to the ^{13}C content of the CO_2 respired in the incubation experiments, due to the potential for microbial fractionation during the incubation experiments.

Formatted: Font: 11 pt

Formatted: Font: 11 pt

Formatted: Header

309 -4.0‰ (Table 2):

310 Table 2. $\delta^{13}\text{C}$ -VPDB‰ signature of the CO_2 evolved from each RO temperature fraction and
311 the incubation experiments in Houston et al. (2024b). Errors are reported to one standard
312 deviation from the mean. (2024).

	$\delta^{13}\text{C}$ -VPDB‰					Incubations (Houston et al., 2024b)
	150-325°C	325-425°C	425-500°C	500-650°C	650-800°C	
T1 0.5 cm	-24.7 ± 0.1	-22.3 ± 0.1	-20.2 ± 0.1	-13.9 ± 0.1	-5.6 ± 0.1	-23.3 ± 0.4
T1 5.5 cm	-26.7 ± 0.1	-24.7 ± 0.1	-22.7 ± 0.1	-21.3 ± 0.1	-6.3 ± 0.1	-23.6 ± 0.4
T1 18.5 cm	-25.9 ± 0.1	-24.0 ± 0.1	-22.6 ± 0.1	-21.6 ± 0.1	-9.5 ± 0.1	-6.1 ± 0.1
T2 0.5 cm	-25.7 ± 0.1	-23.6 ± 0.1	-22.0 ± 0.1	-19.9 ± 0.1	-4.7 ± 0.1	-22.9 ± 0.4
T2 5.5 cm	-26.5 ± 0.1	-24.8 ± 0.1	-23.0 ± 0.1	-22.0 ± 0.1	-21.1 ± 0.1	-23.1 ± 0.4
T2 15.5 cm	-28.0 ± 0.1	-26.6 ± 0.1	-25.4 ± 0.1	-24.4 ± 0.1	-4.0 ± 0.1	-20.2 ± 0.4
T3 0.5 cm	-25.3 ± 0.1	-23.7 ± 0.1	-22.0 ± 0.1	-18.7 ± 0.1	-4.1 ± 0.1	-20.6 ± 0.4
T3 5.5 cm	-26.2 ± 0.1	-24.2 ± 0.1	-22.6 ± 0.1	-20.5 ± 0.1	-12.6 ± 0.1	-23.4 ± 0.4
T3 19.5 cm	-26.3 ± 0.1	-24.2 ± 0.1	-22.6 ± 0.1	-21.2 ± 0.1	-8.0 ± 0.1	-3.7 ± 0.1

314 3.3.4. Ramped oxidation and incubation comparison

315 Figure 14 presents a comparison of the ^{14}C content of the CO_2 evolved from RO temperature
316 fractions (this study) and respired CO_2 from the same soils during aerobic laboratory incubations
317 (Houston et al. 2024b). These comparisons show that for each of the 0.5 cm depth samples,
318 the ^{14}C content of the respired CO_2 was greater than the ^{14}C content of the CO_2 evolved from the
319 same soils in any of the RO temperature fractions in the same soils (Fig. 14). For the 5.5 cm depth
320 samples, the ^{14}C content of the CO_2 respired in the incubations was approximately equivalent to
321 the ^{14}C content of the CO_2 evolved from the 150-325°C RO temperature fraction (Fig. 14). For T2
322 15.5 cm, the ^{14}C content of the respired CO_2 was also closest to the 150-325°C RO temperature
323 fraction (Fig. 14). For the T1 18.5 cm and T3 19.5 cm samples, the ^{14}C contents of the incubation
324 CO_2 were depleted relative to the 150-325°C RO temperature fraction for both samples, and
325 instead, were closest to the 325-425°C and 425-500°C RO temperature fractions, respectively
326 (Fig. 14).

327 3.4. Activation Energy

328 Mean activation energy (μE) ranged from 157.50-170.97 kJ/mol for the 0.5 cm depth samples,
329 159.97-165.32 kJ/mol for the 5.5 cm depth samples, and 154.38-160.44 kJ/mol for the deepest
330 samples (T1 18.5 cm, T2 15.5 cm, T3 19.5 cm, Table 3). The standard deviation of activation energy
331 (σE) ranged from 23.16-35.83 kJ/mol for the 0.5 cm depth samples, 22.16-25.25 kJ/mol for the 5.5

Formatted: Plain Table 5

cm depth samples, and 21.43-23.51 kJ/mol for the deepest samples (Table 3). Between the three depth increments, there were no significant changes in μE , σE , nor activation energy distribution (p (o,E) (

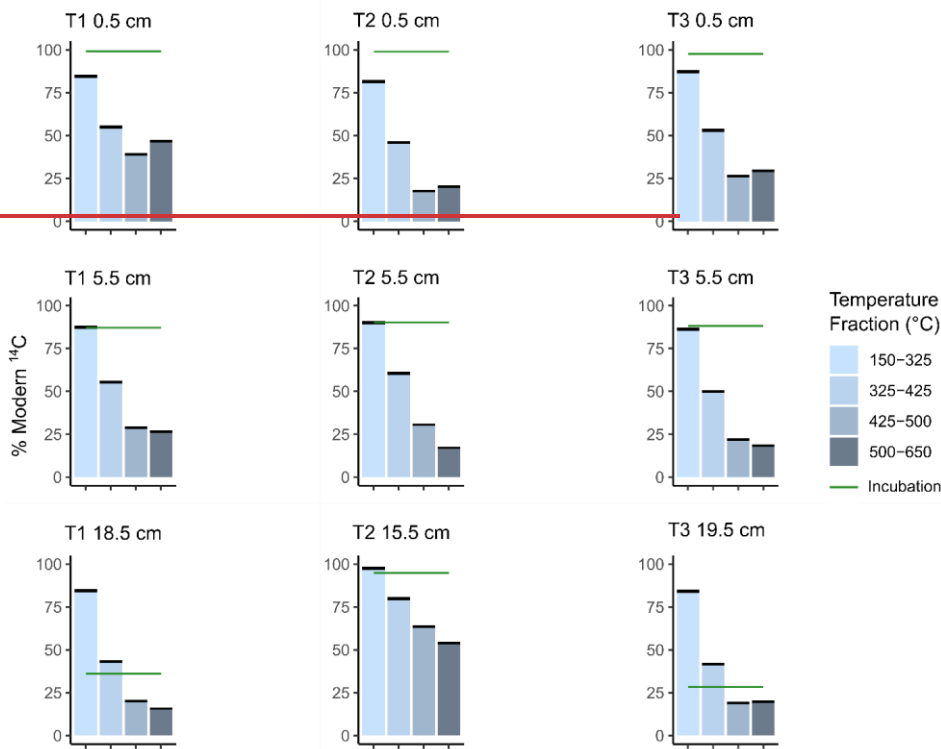


Table 1. ANOVA; p = 0.47, 0.37, and 0.14, respectively).

Table 3. Mean activation energy (μE), standard deviation of activation energy (σE), and activation energy distribution for each sample.

	μE (kJ/mol)	σE (kJ/mol)	p (oE)
T1 0.5 cm	170.97	35.83	0.02
T1 5.5 cm	159.97	22.16	0.02
T1 18.5 cm	160.44	22.72	0.02
T2 0.5 cm	160.47	23.16	0.02
T2 5.5 cm	165.32	25.25	0.01
T2 15.5 cm	154.38	21.43	0.02
T3 0.5 cm	157.50	24.01	0.02

Formatted: Font: Aptos, Font color: Black, Ligatures: None

Formatted: Header

|

341

342

343

344

345

346

347

348

349

350

351

T3 5.5 cm	162.31	24.44	0.02
T3 19.5 cm	160.13	23.51	0.02

Table 4 shows μE and the associated σE for each thermal fraction. μE ranged from 131.04-133.23 kJ/mol for 150-325 °C, 156.83-157.78 kJ/mol for 325-425 °C, 176.14-177.79 kJ/mol for 425-500 °C, 185.44-199.19 kJ/mol for 500-650 °C, and 213.06-247.75 kJ/mol for 650-800 °C (Table 4). σE ranged from 7.33-8.71 kJ/mol for 150-325 °C, 9.83-10.23 kJ/mol for 325-425 °C, 6.88-8.83 kJ/mol for 425-500 °C, 3.68-16.04 kJ/mol for 500-650 °C, and 1.83-10.94 kJ/mol for 650-800 °C (Table 4). μE and σE both varied significantly between the thermal fractions, increasing sequentially (Kruskal-Wallis, $p = 0.001$ and 0.001 , respectively). We therefore infer that the thermal recalcitrance of RO fractions is greater at higher temperatures and use temperature as a proxy for thermal reactivity herein.

Formatted: Plain Table 5

Formatted: Header

352
353

Table 4. Mean activation energy (μE) and standard deviation of activation energy (σE) for each RO temperature fraction for each sample.

	μE (σE) (kJ/mol)				
	150-325°C	325-425°C	425-500°C	500-650°C	650-800°C
T1 0.5 cm	132.43 (7.33)	157.52 (10.17)	177.79 (7.32)	199.19 (16.04)	242.42 (10.94)
T1 5.5 cm	133.23 (8.07)	157.00 (10.13)	177.07 (7.58)	191.06 (7.87)	213.06 (2.12)
T1 18.5 cm	131.90 (8.62)	157.60 (9.83)	176.93 (7.83)	189.53 (6.70)	239.73 (6.73)
T2 0.5 cm	132.10 (8.21)	157.42 (10.08)	177.23 (7.38)	191.39 (10.62)	226.84 (6.81)
T2 5.5 cm	132.15 (8.71)	157.11 (10.01)	177.68 (8.83)	195.80 (7.95)	224.56 (4.55)
T2 15.5 cm	131.04 (8.46)	156.83 (10.23)	176.69 (6.88)	185.44 (3.68)	247.74 (1.83)
T3 0.5 cm	131.59 (7.48)	157.33 (10.07)	176.14 (7.07)	193.65 (12.46)	231.21 (10.04)
T3 5.5 cm	133.05 (8.28)	157.67 (10.14)	177.19 (7.70)	191.13 (9.11)	236.57 (4.29)
T3 19.5 cm	131.73 (8.38)	157.78 (10.00)	176.71 (7.34)	191.7 (10.53)	232.23 (9.69)

354
355
356
357
358
359
360
361
362
363
364
365
366
367

4. Discussion

Soils are complex mixtures of many different OC sources and ages, with different vulnerabilities ~~4.1.~~ to decomposition and turnover. In this study, we aimed to improve our understanding of the carbon cycling of saltmarsh soils by measuring the ¹³C and ¹⁴C content of thermally-fractionated soil carbon pools, and comparing these results to the ¹⁴C content of biologically evolved CO₂ from the same soils (Houston et al., 2024b).

Thermograms

During ramped combustion, CO₂ evolved at low temperatures is deemed to be more energetically favourable for decomposition than CO₂ evolved at higher temperatures, implying that the reactivity of soil OC decreases with increasing temperature (Peltre et al., 2013; Williams and Plante, 2018). Due to the approximately bimodal thermogram distribution (Fig. 1), we can therefore define the low-temperature CO₂ peak as relatively ‘labile’ and the higher temperature CO₂ peak as ‘recalcitrant’ OC pools (Capel et al., 2006). There were no significant trends between

the proportion of CO_2 evolved from the labile (150-425°C) and recalcitrant (425-650°C) RO fractions for either T1, T2, or T3 (Spearman's rho, $p > 0.05$), limiting what we can infer from the distributions of the thermograms. Despite the lack of statistical significance, for both T1 and T3 the height of the higher temperature (recalcitrant) peak relative to the lower temperature (labile) peak increases with increasing depth. This may be caused by OM degradation throughout the burial process during which microbes degrade soil OM, and preferentially deplete the labile OM pool as more favourable for decomposition, which in turn can result in deeper soils having greater proportions of recalcitrant, microbially derived OC (Luk et al., 2021; Soldatova et al., 2024).

Conversely, for T2 the height of the labile peak increased relative to the recalcitrant peak with increasing depth (Fig. 1). This is likely to be because, as well as the soil burial process and the degradation of OM, all samples were within the soil rooting zone (0-40 cm), which can facilitate the transfer of labile OM from the surface to deep soils (Bernal et al., 2017; Rumpel and Kögel-Knabner, 2011). This process may highlight heterogeneity in these saltmarsh soils and in this case may have introduced new labile OM to the deeper soil samples, which was subsequently captured by the RO procedure for the T2 15.5 cm sample, resulting in the increased labile fraction with depth in core T2 (15.5 cm). Due to the low oxygen conditions in waterlogged saltmarsh soils, decomposition rates are slow, and labile OM can persist for extended time periods compared to aerobic soils (Chapman et al., 2019; McTigue et al., 2021). Hence, it is also feasible that the greater proportion of labile OC at depth for T2 is due to preservation of larger inputs of labile OM compounds at the soil surface during the burial process. The difference in the thermogram distributions with depth between T2, and T1/T3, may highlight heterogeneity across the Skinflats saltmarsh soils, even within the same lower marsh zone.

4.2. ^{14}C content of ramped oxidation CO_2 fractions

The changes with depth between the thermogram CO_2 peaks follow similar trends to the RO- ^{14}C content of the corresponding temperature fractions (Fig. 1, [4.1. Carbon provenance of ramped oxidation \$\text{CO}_2\$ fractions](#)

The first three RO temperature fractions (150-325°C, 325-425°C, 425-500°C) were derived solely from OC sources, as IC begins to breakdown from ca. 550°C (Hemingway et al., 2017b). CO_2 from the 500-650°C and 650-800°C fractions may, however, have been evolved from a mix of OC and IC sources. The IC contents of the studied soils (0.11-0.48%) were low relative to OC contents (4.18-7.71%), and IC makes only 1.95-10.48% of the total soil C pool for these samples (Table A3). Wider μE ranges (mean activation energy of each thermal fraction) and increased bond strength

diversity (σE) compared to the first three RO fractions (Table 4) may have been caused by non-first order decomposition of carbonates (a form of IC) from 550 °C, as first order decomposition kinetics are a requirement for the *rampedpyrox* model (Hemingway et al., 2017b). Hemingway (pers. comm. 16/01/2025) confirmed that due to the low amounts of carbonates in these samples (Table A3) that it would be appropriate to calculate activation energies using the *rampedpyrox* model.

IC could have been removed from our saltmarsh soil samples to allow complete analysis of the soil OC pool, and many R(P)O studies have taken this approach (Bao et al., 2019b; Hemingway et al., 2017b; Luk et al., 2021; Stoner et al., 2023; Williams and Rosenheim, 2015). However, our samples have low IC contents (Table A3), and acid-treatment, which is required to remove IC from samples, can cause losses of labile OC (Bao et al., 2019a). Indeed, in Hemingway et al. (2017), acid treatment of samples prior to RO resulted in a shift of 4 % Modern ^{14}C , which could change one of our samples from having a pre-bomb ^{14}C content to a post-bomb ^{14}C content, or vice-versa. A similar shift in ^{14}C content for our samples could seriously impact the interpretations in our study, and our ability to compare the ^{14}C content of the CO_2 respired from bulk (untreated) soils in the incubation experiments (Houston et al., 2024) to the ^{14}C content of the RO fractions. The soils in the incubation experiments were also not decarbonated as the acid-treatment would have affected soil respiration processes and made the results incomparable to in-situ soil degradation processes (Houston et al., 2024b).

4.2. ^{14}C content of ramped oxidation CO_2 fractions

Table 1). For T1 and T3, the increasing proportion of evolved CO_2 -associated with the recalcitrant (high temperature) peak corresponds to a decrease in RO- ^{14}C content (Fig. 1), i.e., the increase in the amount of CO_2 evolved from a recalcitrant pool corresponds to an increase in its age. For T2, the opposite is observed; the decreasing proportion of the evolved CO_2 -associated with the recalcitrant (high temperature) peak corresponds to an increase in RO- ^{14}C content (Fig. 1), i.e., the increase in the amount of CO_2 evolved from the recalcitrant pool corresponds to a decrease in its age. This may suggest the input of a different source of younger but recalcitrant (allochthonous) material in T2. As saltmarsh soil accumulates, and OC is buried and degraded, our data show that the proportion of aged, recalcitrant OC tends to increase with depth, while comparatively younger, labile OC pools also persist.

The ^{14}C -RO content decreased over the four thermal fractions (150-325 °C, 325-425 °C, 425-500 °C, 500-650 °C. Fig. 1 exponentially with increasing temperature (Fig. 2), implying that ^{14}C -depleted the CO_2 evolved from labile (low temperature) OC had a greater thermal recalcitrance

433 than ¹⁴C-enriched OC for these saltmarsh soil samples¹⁴C content than the CO₂ evolved from
434 recalcitrant (high temperature) OC. Since the ¹⁴C content of each RO fraction was
435 <100 % Modern (Fig. 2 Table 1), each of the OC reactivity pools were likely to be predominantly
436 composed of carbon sequestered from the atmosphere before the 1963 ¹⁴C bomb-spike caused
437 by atmospheric nuclear weapons testing, although we cannot completely discount some
438 contributions from post-bomb carbon (Hajdas et al., 2021). Nevertheless, using ¹⁴C content as
439 an estimate of the age of the OC we can infer that the older (¹⁴C-depleted) OC has a greater
440 thermal recalcitrance than young OC carbon reactivity decreases with increasing age for these
441 samples, which. This finding is consistent with previous studies on the thermal reactivity of
442 carbon stored in soils and sediments (e.g., Bao et al., 2019b; Luk et al., 2021; Plante et al., 2013;
443 Stoner et al., 2023) (Bao et al., 2019; Luk et al., 2021; Plante et al., 2013; Stoner et al., 2023).

444 The results suggest inhomogeneity within at least one of the temperature fractions for each
445 sample as, although there were no post-bomb ¹⁴C contents for the incubation or RO samples
446 (Table 1), there is likely to be a fraction of post-bomb (post-AD1955) OC in at least one of the
447 temperature fractions. Autochthonous This is due to autochthonous OC sequestration (post-
448 bomb) at this accreting saltmarsh (Hajdas et al., 2021; Smeaton et al., 2024) which may become
449 obscured by contributions from pre-bomb (pre-AD1955) OC. Observing the exponential decline
450 in ¹⁴C content with increasing temperature (Fig. 12), we hypothesise that, if present, this mixing
451 of pre- and post-bomb C most likely occurred in the 150-325°C fraction. As ¹⁴C content decreases
452 with increasing temperature for the RO fractions, CO₂ with ¹⁴C content greater than any of the
453 measured RO fractions would be expected to have been evolved within the lowest temperature
454 fraction (150-325°C).

455 As the oldest (most ¹⁴C-depleted) C had the greatest thermal recalcitrance (Fig. 1), this
456 emphasises that saltmarshes accumulating greater amounts of older (¹⁴C-depleted) OC will
457 likely provide the most thermally recalcitrant OC stores, and saltmarshes accumulating greater
458 proportions of contemporary OC, either through in-situ production or young allochthonous
459 components, contain soil OC stores which are of greater thermal lability (Komada et al., 2022;
460 Van de Broek et al., 2018). However, the ¹⁴C contents of the lowest temperature RO fraction (81-
461 98 % Modern; Table 1) highlight that although the thermal reactivity of OC decreases with ¹⁴C
462 content (Fig. 1), thermally labile OC can still be aged (at least hundreds of years old) for these
463 soils. Due to the often anaerobic and non-eroding conditions of buried sediments, saltmarshes
464 can therefore be stores of old, but thermally labile carbon. Of course, the thermal recalcitrance
465 of OC is not necessarily related to biological turnover time, as this is also dependent on the
466 prevailing environmental conditions (Schmidt et al., 2011; Spivak et al., 2019).

Formatted: Plain Table 5

Formatted: Font: +Body (Aptos)

Field Code Changed

Formatted: Font: +Body (Aptos)

Field Code Changed

Formatted: Header

The ^{14}C -RO contents ranged from $97.53 \pm 0.50\%$ Modern for T2 15.5 cm in the 150-325°C fraction to $15.70 \pm 0.12\%$ Modern for T1 10.5 cm (Table 1), highlighting the role of saltmarshes both as stores of contemporary and highly aged carbon as these ^{14}C contents correspond to conventional radiocarbon years BP (relative to AD 1950) of 201 ± 41 years BP and $14,875 \pm 61$ years BP, respectively (Table A2). While regional deglaciation of this part of Scotland is likely to postdate the age of $14,875 \pm 61$ years BP (Ballantyne and Small, 2019), we note that the catchment geology contains sources of petrogenic carbon (Miller et al., 2023), which would be ^{14}C -dead and may have diluted the ^{14}C content of the highest temperature RO- CO_2 fractions. As the oldest carbon was stored in the lowest reactivity fraction (Fig. 2), this emphasises that saltmarshes accumulating greater amounts of pre-aged OC will likely provide the most stable OC stores, and saltmarshes accumulating greater proportions of contemporary OC, either through in-situ production or young allochthonous components, contain soil OC stores which are of greater vulnerability for remineralisation and loss to the atmosphere (Komada et al., 2022; Van de Broek et al., 2018). However, the ^{14}C contents of the 150-325°C fraction ($81\text{--}98\%$ Modern) correspond to uncalibrated ^{14}C ages of $201\text{--}1643$ years BP (SI), highlighting that although OC reactivity decreases with age (Fig. 2), the labile OC fraction can still be centuries to millennia in age for these soils and that, due to the often anaerobic and non-eroding conditions of buried sediments, saltmarshes can be stores of old, but reactive, carbon.

4.3. ^{13}C content of ramped oxidation CO_2 fractions

^{13}C -RO increased sequentially with the thermal fractions (Fig. 2), due to greater contributions from relatively ^{13}C -enriched C sources from the higher temperature thermal fractions. The ^{13}C -RO contents of the 150-650 °C fractions were each typical of OC sources (Leng and Lewis, 2017), whereas the ^{13}C -RO contents of the 650-800 °C fraction were mostly typical of at least a partial contribution from an IC source, with the exception of T2 5.5 cm and T3 5.5 cm (Table 2) (Brand et al., 2014; Ramnarine et al., 2012). As IC can begin to evolve from 550 °C, it is possible that a mix of OC and IC sources was present in the 500-650 °C thermal fractions.

As ^{13}C -RO increased with temperature (Fig. 2, Table 2), ^{13}C -enriched OC had a greater thermal recalcitrance than ^{13}C -depleted OC for these samples. Previous work has demonstrated that $>80\%$ of the OC accumulating at Skinflats saltmarsh is autochthonous/terrestrial in origin (Miller et al., 2023), with limited contributions from marine OC. The thermally recalcitrant OC was potentially composed of a greater amount of OC which has undergone microbial decomposition as this process tends to enrich the degraded OC in ^{13}C (Boström et al., 2007; Etcheverría et al., 2009; Luk et al., 2021; Sanderman and Grandy, 2020; Soldatova et al., 2024; Stoner et al., 2023).

Formatted: Plain Table 5

Formatted: Font: +Body (Aptos), 11 pt

Formatted: Justified

Formatted: Header

The thermally recalcitrant OC may instead/also have been composed of more different OM compounds (e.g., lignins, aromatics) than the more thermally labile OC (e.g., carbohydrates, lipids) (Sanderman and Grandy, 2020). It is also possible that methodological artefacts, such as kinetic fractionation, influenced the ^{13}C -RO contents. Kinetic fractionation is explained by different carbon isotopes evolving as CO_2 from the soil sample at different rates during the ramped heating (Hemingway et al., 2017a). Kinetic fractionation would cause the ^{13}C content of the evolved CO_2 to increase linearly with temperature (Hemingway et al., 2017a), and we cannot rule out this artefact. Hemingway et al. (2017a) determined that kinetic fractionation was not an important factor in their RPO procedure, but we used a different set-up (described in Garnett et al., 2023).

$\delta^{13}\text{C}$ -RO also had a significant trend with temperature, increasing linearly (Fig. 3). Therefore, thermally recalcitrant OC (oxidised at high temperatures) tended to be ^{13}C enriched compared to labile OC. This implies that the recalcitrant OC was likely to be composed of a greater amount of OC which has undergone microbial decomposition as this process tends to enrich the degraded OC in ^{13}C (Boström et al., 2007; Etcheverría et al., 2009; Luk et al., 2021; Sanderman & Grandy, 2020; Soldatova et al., 2024; Stoner et al., 2023). It is also possible that methodological artefacts, such as kinetic fractionation, influenced the ^{13}C -RO contents. Kinetic fractionation is explained by different carbon isotopes evolving as CO_2 from the soil sample at different rates during the ramped heating (Hemingway et al., 2017). Kinetic fractionation would cause the ^{13}C content of the evolved CO_2 to increase linearly with temperature (Hemingway et al., 2017), as we observed in Fig. 3, so we cannot rule out this artefact.

4.4. Changes in the isotopic content of ramped oxidation CO_2 fractions with depth

The isotopic composition of the evolved CO_2 did not vary significantly with depth for any of the temperature fractions. The lack of an increase in the age (^{14}C -depletion) of soil C with sample depth is unusual, as typically C undergoes a burial process, and previous work has shown diagenetic ageing of saltmarsh soils with depth as young OC is turned over faster than old OC (Komada et al., 2022; Van de Broek et al., 2018).

Compared to other UK saltmarshes, Skinflats has relatively high C accumulation rates (Miller et al., 2023; Smeaton et al., 2024). Depleted ^{14}C contents of the OC accumulating at the Skinflats saltmarsh (Houston et al., 2024b) The range in ^{13}C -RO contents between 150-800°C shows a clear distinction between 150-650°C and 650-800°C (Table 2). There was a strong positive linear relationship between ^{13}C content and temperature for the 150-650°C range (Fig. 3), which was not the case for the 650-800°C range as the ^{13}C contents of the CO_2 evolved from the 500-650°C

to the 650–800°C range increases in a non-linear manner (Table 2). This is likely to be because the C-pools from 150–650°C are mostly composed of OC, whereas the 650–800°C pool is mostly composed of IC. We deemed this to be the case as the ^{13}C contents of the CO_2 evolved between 150–650°C were typical of OC sources (Leng et al., 2006; Leng & Lewis, 2017), whereas the ^{13}C contents of the CO_2 evolved between 650–800°C were mostly typical of at least a partial contribution from an IC source, with the exception of T2 5.5 cm and T3 5.5 cm (Table 2) (Brand et al., 2014; Ramnarine et al., 2012).

The CO_2 evolved from 650–800°C for T1 0.5 cm had a ^{13}C content of -5.6‰ , indicating that it was from a predominantly IC source. Given the ^{14}C content was $79.75 \pm 0.37\text{‰}$ Modern, we determined that this was likely to be from a biogenic IC source, potentially shell fragments.

~~4.4~~ Comparison of biologically and thermally evolved CO_2

For these saltmarsh soils, thermally recalcitrant OC was ^{13}C -enriched and ^{14}C -depleted compared to thermally labile OC. This implies that labile OC tends to be relatively young compared to recalcitrant OC which tends to be composed of more degraded and aged OC. These findings are consistent with a previous study on the thermal reactivity (using ramped pyrolysis oxidation) of saltmarsh soil OM (Luk et al., 2021) and other soil and sediment OM studies (Sanderman and Grandy, 2020; Stoner et al., 2023).

We did not attempt to relate the ^{13}C -RO to the ^{13}C content of the CO_2 respired in the incubation experiments, due to the potential for microbial fractionation during the incubation experiments. Microbial alteration can change the ^{13}C content of the respired CO_2 and the resulting soil OC (Soldatova et al., 2024; Werth and Kuzyakov, 2010), so it is possible that the CO_2 collected for isotopic analysis in Houston et al. (2024) did not reflect the ^{13}C content of the OC pool it was respired from. Therefore, the ^{13}C content of the biologically evolved CO_2 and the ^{13}C -RO measured in this study are not comparable. We focus the remainder of our discussion on comparing the ^{14}C content of the biologically evolved CO_2 (Houston et al., 2024) to ^{14}C -RO measured in this study, which would not be affected by microbial fractionation during the incubation period (^{14}C results are normalised using the measured $\delta^{13}\text{C}$ values and therefore corrected for isotopic fractionation).

Fig. 4 shows that for each of the 0.5 cm depth samples, the ^{14}C content of the CO_2 respired in the aerobic laboratory experiments was ^{14}C -enriched relative to any of the RO temperature fractions, which was also the case for the T3 5.5 cm sample (Table 1). This was likely to be caused by inhomogeneity in the OC reactivity pools, as each defined thermal reactivity pool may be composed of multiple OC sources of variable age and composition. Due to the negative

exponential relationship between $^{14}\text{CO}_2\text{-RO}$ and temperature (Fig. 2), we hypothesise that for soil samples producing respired CO_2 that was ^{14}C -enriched relative to any of the RO fractions (T1 0.5 cm, T2 0.5 cm, T3 0.5 cm, T3 5.5 cm; Table 1, Fig. 4), that this CO_2 was biologically produced from an OC pool within the most thermally labile RO fraction (150–325°C). Thus, we suggest that even within the 150–325°C RO fraction there are pools of even younger OM, but that they are masked by older, ^{14}C -depleted OM. This implies that RO- ^{14}C analysis of finer temperature fractions could provide further insights into the turnover of young carbon in these soils.

The ^{14}C content of respired CO_2 from the 5.5 cm depth samples tended to be closer to the ^{14}C content of the lowest temperature (150–325°C) RO fraction (Fig. 4), implying that for these samples the biologically evolved CO_2 was from a thermally labile OC pool. The T2 15.5 cm respired CO_2 sample was also similar in ^{14}C content to the lowest temperature RO fraction, whereas respired CO_2 from the slightly deeper T1 18.5 cm and T3 19.5 cm samples was ^{14}C -depleted relative to the 150–325°C RO fraction, instead aligning closer to the higher temperature RO fractions (Fig. 4). This implies that the biologically evolved CO_2 from T1 18.5 cm and T3 19.5 cm was not from a thermally labile OC pool. The ^{14}C content of the CO_2 evolved from the aerobic incubations of T1 18.5 cm and T3 19.5 cm was hypothesized to have been evolved from an inorganic C source due to the enriched ^{13}C contents of -6.1‰ and -3.7‰, respectively (Houston et al., 2024). As IC reactivity is controlled by different factors than OC reactivity (Van Dam et al., 2021), and the remainder of the samples were determined to evolve from OC substrates, this is likely to explain why the ^{14}C content of the CO_2 evolved from the aerobic incubation experiments for T1 18.5 cm and T3 19.5 cm did not align with the lowest temperature (most thermally labile) RO fraction (Fig. 4). Therefore, there was a clear depth trend in the relationship between the ^{14}C content of CO_2 respired in the aerobic incubation experiments and the ^{14}C content of the CO_2 evolved during RO of the same bulk soils.

The depleted ^{14}C contents of some of the OC accumulating at the Skinflats saltmarsh (201 ± 41 years BP to 14,875 ± 61 years BP; Table A2) imply that a proportion of the OC being buried may already have been pre-aged at the time of deposition on the marsh surface, as the marsh formed in the 1930's (Miller et al., 2023). The combination of high carbon accumulation rates and depleted soil ^{14}C contents implies that the Skinflats saltmarsh accumulates a high proportion of old, most likely allochthonous OC. Some of the aged, allochthonous OC may have undergone significant microbial processing and degradation prior to its accumulation in the saltmarsh soil. As the OM is degraded, and the energetically favourable components are consumed, the resulting OM becomes increasingly thermally. This means that some of the OC may have undergone significant microbial processing and degradation prior to its accumulation in the

Formatted: Plain Table 5

Formatted: Font: 11 pt

Formatted: Font: +Body (Aptos)

Formatted: Header

saltmarsh soil. It is also possible that highly aged OC could remain labile if it had been stored in an environment with low rates of microbial decomposition, e.g., a peatland (Dean et al., 2023). Regardless of the age and degradation state of the OC deposited onto the marsh surface, as it gets buried it will undergo a degree of microbial processing and degradation in the saltmarsh soil (Luk et al., 2021). As the OM is degraded, and the energetically favourable components are consumed, the resulting OM becomes increasingly recalcitrant (Luk et al., 2021; Sanderman and Grandy, 2020; Soldatova et al., 2024). The accumulation of a high proportion of degraded OC on the Skinflats saltmarsh may therefore explain the lack of observed change in the isotopic composition of the soil OC pools with depth. Therefore, at depth we would expect to see an increase in the relative proportion of recalcitrant OC, which we do for T1 and T3 (Fig. 1). The in-situ degradation of soil OM may reduce these inhomogeneities with depth as the labile OM components either get consumed or degraded to a recalcitrant (higher RO temperature) state. We did not measure fine-scale changes in RO-¹⁴C content within the 150-325°C temperature window for any of the samples, but if this is the case, there would be less of a range of ¹⁴C contents within the 150-325°C RO fraction for the 5.5 cm and deeper samples than for the 0.5 cm samples.

Not all old OC is degraded or thermally recalcitrant, and our results show that the Skinflats saltmarsh is also a store of old (¹⁴C-depleted), thermally labile OC (Fig. 1). Old OC can be thermally labile if it 'ages' (is stored) in an environment with low decomposition rates, e.g., a peatland (Dean et al., 2023), prior to transport and accumulation into the saltmarsh. There are extensive peatlands in the Skinflats catchment, many of which are degrading (Lilly et al., 2012). Regardless of the age and degradation state of the OC deposited onto the marsh surface, as it gets buried it will undergo a degree of microbial processing and degradation in the saltmarsh soil (Luk et al., 2021), but that process is potentially less prevalent at Skinflats than saltmarshes accumulating younger, less degraded OC.

Through isotopic analysis of saltmarsh soils partitioned using ramped oxidation, we have determined that increased thermal recalcitrance is related to older (¹⁴C-depleted; Fig. 1), more degraded/microbially derived (¹³C-enriched; Fig. 2) soil C. These findings are consistent with previous research on the thermal reactivity of soil and sediment C, that more energy is required (higher temperature/μE) to decompose older (¹⁴C-depleted), degraded/microbially derived (¹³C-enriched) C than younger (¹⁴C-enriched), less processed (¹³C-depleted) C (e.g., Bao et al., 2019b; Plante et al., 2013; Stoner et al., 2023), including one saltmarsh study (Luk et al., 2021).

Formatted: Plain Table 5

Formatted: Font: +Body (Aptos)

Field Code Changed

Formatted: Default Paragraph Font

Formatted: Header

631 **4.5. Comparison of biologically and thermally evolved CO₂**
632 As the biological turnover time of OC depends on the prevailing environmental conditions as well
633 as thermal reactivity (Schmidt et al., 2011), the isotopic composition of the most biologically- and
634 thermally-reactive saltmarsh soil OC pools may not be the same. To determine if this is the case,
635 or not, we compared the isotopic composition of the RO thermal reactivity fractions to the
636 isotopic composition of the CO₂ that was evolved biologically during incubations of equivalent
637 samples (Houston et al., 2024b) (Fig. 1).

638 Figure 1 shows that for each of the 0.5 cm depth samples, the ¹⁴C content of the CO₂ respired in
639 the aerobic laboratory experiments was ¹⁴C-enriched relative to any of the RO temperature
640 fractions, which was also the case for the T3 5.5 cm sample (Table 3). The relative ¹⁴C-enrichment
641 of the biologically respired CO₂ compared to the thermally evolved CO₂ was likely caused by
642 inhomogeneity in the OC thermal reactivity pools, as each defined thermal reactivity pool may be
643 composed of multiple OC sources of variable age and composition. As thermal recalcitrance is
644 related to ¹⁴C-depletion for these samples (Fig. 1), we hypothesise that for saltmarsh soil samples
645 producing respired CO₂ that was ¹⁴C-enriched relative to any of the RO fractions (T1 0.5 cm, T2
646 0.5 cm, T3 0.5 cm, T3 5.5 cm; Table 1, Fig. 1), that this CO₂ was biologically-produced from an OC
647 pool within the most thermally labile RO fraction (150-325°C). Thus, we suggest that even within
648 the 150-325 °C RO fraction there are pools of even younger OC, but that they are masked by older,
649 ¹⁴C-depleted OC.

650 The ¹⁴C content of respired CO₂ from the 5.5 cm depth samples tended to be closer to the ¹⁴C
651 content of the lowest temperature (150-325°C) RO fraction (Fig. 1), implying that for these
652 samples the biologically evolved CO₂ was from a thermally labile OC pool. The T2 15.5 cm
653 respired CO₂ sample was also similar in ¹⁴C content to the lowest temperature RO fraction,
654 whereas respired CO₂ from the slightly deeper T1 18.5 cm and T3 19.5 cm samples was ¹⁴C-
655 depleted relative to the 150-325°C RO fraction, instead aligning closer to the higher temperature
656 RO fractions (Fig. 1). The biologically evolved CO₂ from T1 18.5 cm and T3 19.5 cm was therefore
657 not from a thermally labile OC pool. The ¹⁴C content of the CO₂ evolved from the aerobic
658 incubations of T1 18.5 cm and T3 19.5 cm was hypothesized to have been derived from an
659 inorganic C source due to the enriched ¹³C contents of -6.1‰ and -3.7‰, respectively (Houston
660 et al., 2024b). As IC biological turnover times are controlled by different factors than OC, (Van
661 Dam et al., 2021), and the remainder of the samples were determined to evolve from OC
662 substrates, this is likely to explain why the ¹⁴C content of the CO₂ evolved from the aerobic
663 incubation experiments for T1 18.5 cm and T3 19.5 cm did not align with the lowest temperature

Formatted: Plain Table 5

Formatted: Font: 11 pt

Formatted: Font: +Body (Aptos)

Formatted: Header

(most thermally labile) RO fraction (Fig. 1). Therefore, there was a clear depth trend in the relationship between the ^{14}C content of CO_2 respired in the aerobic incubation experiments and the ^{14}C content of RO fractions of the same bulk soils. Degradation of the thermally labile OM components to a more thermally recalcitrant state during burial may reduce the inhomogeneities within the most thermally labile RO fraction for this study.

For seven out of nine samples (T1 18.5 cm and T3 19.5 cm being the outliers), the ^{14}C content of the CO_2 evolved from the aerobic laboratory incubations was closest to the ^{14}C content of the 150-325°C RO temperature fraction. Therefore, even though the CO_2 evolved from the aerobic incubation experiments was determined to be from a predominantly aged, allochthonous OC source (Houston et al., 2024b)(Houston et al., 2024), it can now also be shown to be derived from a predominantly thermally labile OC pool (Fig. 1).

We did not attempt to relate the ^{13}C -RO to the ^{13}C content of the CO_2 respired in the incubation experiments, due to the potential for microbial fractionation during the incubation experiments 4). The results from our study suggest that saltmarshes can be stores of old, labile OC which can change the ^{13}C content of the respired CO_2 and the resulting soil OC (Soldatova et al., 2024; Werth and Kuzyakov, 2010). In contrast, ^{14}C results are normalised using the measured $\delta^{13}\text{C}$ values and are therefore immune to such isotopic fractionation effects.

4.6. Implications

Our results show that aged (presumed allochthonous), thermally labile OC stored in saltmarsh soils remains vulnerable to remineralisation and loss to the atmosphere upon habitat drainage. Saltmarsh soils usually exist in low-oxygen, tidally-inundated conditions which slow decomposition of OC (Chapman et al., 2019), but many saltmarshes globally have been in oxic conditions, e.g. when a saltmarsh is drained (and their soils subsequently oxidised) to convert them for land uses such as housing developments and agriculture (Bromberg and Bertness, 2005; Campbell et al., 2022; Morris et al., 2012). In the Forth Estuary, where the Skinflats saltmarsh is located, as much as 50% of the intertidal area has been converted to agricultural land since 1600, often involving the drainage of saltmarshes (Hansom and McGlashan, 2008). or the soils disturbed:

Protecting saltmarshes from degradation following drainage is listed as an eligible activity for generating carbon credits for blue carbon ecosystem (BCE) projects (VERRA, 2023) and there is significant potential for climate mitigation by avoided emissions from protecting vulnerable stocks of soil OC in BCEs (Goldstein et al., 2020; Griscom et al., 2017; Kwan et al., 2025; Sasmito et al., 2025). Similarly, the re-creation of saltmarsh habitat through managed realignment (rewetting by tidal inundation) of historic saltmarsh habitats which were previously reclaimed for

land use purposes (e.g., agriculture) could reduce (and possible reverse) the emissions of aged OC to the atmosphere, both locally to Skinflats, and globally.

The evidence for the respiration of thermally labile, allochthonous OC from saltmarsh soils in a drainage degradation scenario demonstrates that at least this fraction of allochthonous OC should be counted as additional in carbon crediting projects and National GHG Inventories. Because allochthonous OC can account for up to 90 % of saltmarsh soil carbon (Komada et al., 2022), the inclusion of allochthonous OC (or even a fraction of it) would significantly increase the climate mitigation awarded to blue carbon projects (as carbon credits, or contributions to National GHG Inventories) (Houston et al., 2024a).

As the bioavailable OC respired in the experiments of Houston et al. (2024b) was (in most cases) from a predominantly thermally labile OC pool, and ^{14}C -RO decreased (C became older) with increasing temperature (thermal recalcitrance), RO measurements could be useful for characterising the turnover times of OC pools for saltmarsh soils exposed to oxic conditions (drainage degradation scenario). The use of thermally defined OC pools to characterize OC turnover times for saltmarsh soils would require a modelling advancement to constrain degradation rates and residence times. Such efforts are not within the scope of this study but could inform additionality/permanence in these saltmarsh systems. Experimentally defined turnover times of OC thermal reactivity pools could, for example, provide a more robust approach than inclusion/exclusion of allochthonous OC from saltmarsh 'blue carbon' projects (Houston et al., 2024a).

Further research is needed to determine if the relationship between biological and thermal lability exists for different degradation scenarios such as nutrient enrichment, as OC turnover time depends on the environmental conditions as well as the thermal lability of the OC pools. Similarly, these experiments would need to be replicated for a wider range of saltmarshes (high and low latitude saltmarshes, different typologies), as there are likely to be differences in OC turnover in different systems.

The samples used for this study were from the low marsh zone only, but it is likely that the thermal reactivity of the Skinflats saltmarsh soil C will vary spatially across the marsh, as the proportion of OC sources has been shown to be variable across saltmarshes (Middelburg et al., 1997). Given our findings that old (^{14}C -depleted) OC has greater thermal recalcitrance than young (^{14}C -enriched) OC (Fig. 1), we anticipate that higher marsh zones, which typically have greater proportions of autochthonous OC than lower marsh zones (Spohn et al., 2013), would contain a greater proportion of thermally labile OC. However, it is important to recognise that some of the

730 young (^{14}C -enriched), autochthonous OC in saltmarsh soils can also be thermally recalcitrant.
731 As well as marsh zonation, we expect that the proportion of OC sources (and associated mix of
732 thermal reactivities) would also vary with proximity to marsh creeks which redistribute
733 autochthonous and allochthonous C across the saltmarsh habitat (Middelburg et al., 1997; Reed
734 et al., 1999). In previously published work we showed that Skinflats accumulates OC of a much
735 greater 'age' (depleted soil ^{14}C contents) than two other saltmarshes in Scotland (Houston et al.,
736 2024b).

737 In this paper we have determined that age (^{14}C -content) is related to the thermal recalcitrance of
738 saltmarsh soil OC. We therefore speculate that sites accumulating younger OC would have more
739 thermally labile soil OC than sites accumulating older OC, like Skinflats, with wider implications
740 for the risks to these vulnerable stores of soil carbon from human disturbances.

741 **5. Conclusions**

742 This is the first study on saltmarsh soils to employ the ramped oxidation method. We show that
743 old (^{14}C -depleted ~~(up to 14,875 years BP)~~) carbon dominates the thermally recalcitrant OC pools.
744 The thermally ~~, whereas the~~ labile OC pools are also aged (^{14}C -depleted) compared to the
745 contemporary atmosphere but are ~~composed of~~ younger than the thermally recalcitrant OC
746 pools. ~~(201-1843 years BP) carbon.~~ These results highlight the role of saltmarshes as mixed stores
747 of both old, thermally recalcitrant OC, as well as younger, thermally ~~old~~, labile OC.

748 We present the first comparison of the bioavailability (CO_2 evolved from incubation experiments;
749 Houston et al., 2024)) and the thermal reactivity (RO) of saltmarsh soil OC. We show that pre-
750 aged, allochthonous CO_2 evolved from saltmarsh soils exposed to oxic conditions (Houston et
751 al., 2024b)(Houston et al., 2024) are from a predominantly thermally labile OC pool. As saltmarsh
752 soils exist mostly in low oxygen, waterlogged conditions, management interventions to limit their
753 exposure to elevated oxygen availability may protect and conserve these stores of thermally ~~old~~,
754 labile OC and provide a climate abatement service. Therefore, we recommend that thermally
755 labile allochthonous OC stored in saltmarsh soils should be counted as additional in some
756 carbon crediting projects and National GHG Inventories.

757 **Appendix A**

758 *Table A1. Additional ^{14}C measurement from the 650-800 °C. ^{14}C was measured at the Scottish*
759 *Universities Environmental Research Centre Accelerator Mass Spectrometer (AMS) Laboratory.*
760 *$\delta^{13}\text{C}$ (relative to Vienna PDB standard) was measured using isotope ratio mass spectrometry on*
761 *a Delta V (Thermo, Germany) and used to normalize the ^{14}C results to a $\delta^{13}\text{C} = -25\text{‰}$, which*

Formatted: Plain Table 5

Formatted: Justified

Formatted: Font: +Body (Aptos), 11 pt, Font color: Auto

Formatted: Heading 1, Left, Line spacing: single

Formatted: Header

762 were reported as %Modern ¹⁴C (i.e., Fraction modern × 100). Errors are reported to one
763 standard deviation from the mean.

764 Table A1. Percentage of CO₂ evolved during ramped oxidation of each sample from the labile (150-425°C) and
765 recalcitrant 388 (425-650°C) temperature ranges:

Sample ID	% Modern ¹⁴ C Labile (150-425°C)	Recalcitrant (425-650°C)
Skin T1 0.5 cm 650-800 °C	79.75 ± 0.5059.54	40.46
T1 5.5 cm	62.99	37.01
T1 18.5 cm	60.12	39.88
T2 0.5 cm	57.53	42.47
T2 5.5 cm	50.00	50.00
T2 15.5 cm	64.07	35.93
T3 0.5 cm	64.97	35.03
T3 5.5 cm	59.61	40.39
T3 19.5 cm	64.86	35.14

766
767 Table A2. Isotopic compositions measured by IRMS ($\delta^{13}\text{C}$) compared to values estimated by the
768 ramped pyrox model (Hemingway, 2016). Modelled and measured $\delta^{13}\text{C}$ values are significantly
769 different (Mann-Whitney-U test, $p = 0.04$).

770 Table A2. Conventional radiocarbon age (years BP, where 0 BP = AD 1950 and age = $-8033 \times \ln(\% \text{Modern}/100)$) for each
771 of the samples. Measurement errors are reported to one standard deviation (1 σ). We also report the amount of CO₂
772 evolved from each temperature fraction from which CO₂ was collected for ¹⁴C measurement, reported as %Carbon:

Sample ID	$\delta^{13}\text{C}$ (measured) Radio carbon Age (years BP)	$\delta^{13}\text{C}$ (modelled) Radi ocarbon Age 1 σ uncertainty	%Carbon
Skin T1 0-1cm-5 cm 150-325 °C	-24.7 ± 0.1,344	42	-30.1 ± 0.2-42
Skin T1 0-1cm-5 cm 325-425 °C	-22.3 ± 0.14,800	-27.8 ± 0.243	1.17
Skin T1 0-1cm-5 cm 425-500 °C	-20.2 ± 0.17,527	-25.6 ± 0.242	1.07
Skin T1 0-1cm-5 cm 500-650 °C	-13.9 ± 0.16,108	44	-19.5 ± 0.269
Skin T1 0-1cm-5 cm 650-800 °C	-5.6 ± 0.1,818	37	-11.1 ± 0.253
Skin T1 5-6cm-5 cm 150-325 °C	-26.7 ± 0.1,072	-27.7 ± 0.240	1.44
Skin T1 5-6cm-5 cm 325-425 °C	-24.7 ± 0.14,740	-25.8 ± 0.241	1.59
Skin T1 5-6cm-5 cm 425-500 °C	-22.7 ± 0.140,011	-23.8 ± 0.246	1.11
Skin T1 5-6cm-5 cm 500-650 °C	-21.3 ± 0.140,650	-22.6 ± 0.248	0.67
Skin T1 5-6cm 650-800 °C	-6.3 ± 0.1	-8.0 ± 0.2	

[illegible]

Skin T3 0-1cm 650-800 °C				
	-4.1 ± 0.1	-6.2 ± 0.2		
Skin T3 5-6cm-5 cm 150-325 °C	-26.2 ± 0.1	-27.8 ± 0.2	1.13	
				1.32
Skin T3 5-6cm-5 cm 325-425 °C	-24.2 ± 0.15	-25.9 ± 0.24		1.08
Skin T3 5-6cm-5 cm 425-500 °C	-22.6 ± 0.14	-24.3 ± 0.25		0.58
Skin T3 5-6cm-5 cm 500-650 °C	-20.50 ± 0.14	-22.32 ± 0.25		
Skin T3 5-6cm 650-800 °C	-12.60 ± 0.1	-14.29 ± 0.2		
Skin T3 19-20cm-5 cm 150-325 °C	-26.30 ± 0.1	-27.48 ± 0.2		1.75
				1.14
Skin T3 19-20cm-5 cm 325-425 °C	-24.20 ± 0.17	-25.40 ± 0.24		0.64
Skin T3 19-20cm-5 cm 425-500 °C	-22.60 ± 0.14	-23.78 ± 0.25		
Skin T3 19-20cm-5 cm 500-650 °C	-21.20 ± 0.14	-22.57 ± 0.25		
Skin T3 19-20cm 650-800 °C	-8.00 ± 0.1	-9.30 ± 0.2		

Table A3. Soil carbon properties measured on equivalent sub-samples prior to the RO procedure, as reported in Houston et al. (2024). Total organic carbon (TOC), Total carbon (TC) for the soil samples were measured by a SoliTOC analyser (Elementar Analysensysteme, Hanau, Germany). ¹⁴C was measured at the Scottish Universities Environmental Research Centre Accelerator Mass Spectrometer (AMS) Laboratory. δ¹³C (relative to Vienna PDB standard) was measured using isotope ratio mass spectrometry on a Delta V (Thermo, Germany) and used to normalize the ¹⁴C results to a δ¹³C = -25‰, which were reported as %Modern ¹⁴C (i.e., Fraction modern × 100). Errors are reported to one standard deviation from the mean.

Sample ID	TOC (%)	TIC (%)	TC (%)	% Modern ¹⁴ C	δ ¹³ C
SK T1 0.5 cm	4.1	0.48	4.58	47.49 ± 0.23	-23.5 ± 0.1
SK T1 5.5 cm	4.96	0.11	5.06	45.03 ± 0.20	-24.5 ± 0.1
SK T1 18.5 cm	4.8	0.39	5.18	41.36 ± 0.19	-23.8 ± 0.1
SK T2 0.5 cm	4.71	0.16	4.87	31.47 ± 0.15	-22.2 ± 0.1
SK T2 5.5 cm	4.23	0.13	4.36	43.69 ± 0.21	-24.1 ± 0.1
SK T2 15.5 cm	7.56	0.15	7.71	50.93 ± 0.24	-25.1 ± 0.1
SK T3 0.5 cm	5.37	0.12	5.49	47.03 ± 0.22	-23.7 ± 0.1
SK T3 5.5 cm	4.06	0.11	4.18	44.15 ± 0.21	-24.0 ± 0.1
SK T3 19.5 cm	5.23	0.12	5.35	44.48 ± 0.21	-24.1 ± 0.1

Formatted: Plain Table 5

Formatted: Font: Bold

Formatted: Font: Bold

Formatted: Space After: 0 pt, Line spacing: single

Formatted: Font: Bold

Formatted: Font: (Default) Aptos

Formatted: Font: Bold

Formatted: Font: Bold

Formatted: Font: Bold

Formatted: Space After: 0 pt, Line spacing: single

Formatted Table

Formatted: Font: Bold

Formatted: Font: Bold

Formatted: Font: Bold

Formatted: Space After: 0 pt, Line spacing: single

Formatted: Font: Bold

Formatted: Font: Bold

Formatted: Space After: 0 pt, Line spacing: single

Formatted: Font: Bold

Formatted: Space After: 0 pt, Line spacing: single

Formatted: Font: Bold

Formatted: Font: Bold

Formatted: Font: (Default) Aptos

Formatted: Space After: 0 pt, Line spacing: single

Formatted: Font: Bold

Formatted: Font: Bold

Formatted: Font: Bold

Formatted: Space After: 0 pt, Line spacing: single

Formatted Table

Formatted: Font: Bold

Formatted: Font: Bold

Formatted: Font: Bold

Formatted: Space After: 0 pt, Line spacing: single

Formatted: Font: Bold

Formatted: Font: Bold

Formatted: Font: Bold

Formatted: Space After: 0 pt, Line spacing: single

Formatted: Normal, Justified, Don't keep with next

Formatted: Header

783 **Data Availability**

784 All data presented in this manuscript is available in the main text and; appendices, ~~and~~

785 ~~supporting information~~.

786 **Author Contribution Statement**

787 A.H. undertook the study, fieldwork, sample processing, data acquisition, and wrote the first draft

788 of the manuscript. M.G. conducted the laboratory procedures with the help of A.H. A.H., W.A.,

789 and M.G. contributed to designing the study, fieldwork, and laboratory analyses. W.A., M.G., and

790 J.S. oversaw the study and contributed to writing and revision of the manuscript.

791 **Competing Interests**

792 The authors declare that they have no conflict of interest.

793 **Acknowledgements**

794 We thank Jo Smith (University of Aberdeen) for her comments and edits on the first draft of this

795 manuscript. We thank the NERC SUPER DTP for funding the PhD through which this research

796 was undertaken (NE/S007342/1). We acknowledge support from the National Environmental

797 Isotope Facility in funding the ¹⁴C measurements for this study under grant NE/S011587/1

798 (allocation numbers 2594.1022, 2709.1023). WENAWA also acknowledges support provided by

799 the HORIZON-CL5-2023-D1-02-02 grant C-BLUES, Innovation to advance the evidence base for

800 reporting of Blue Carbon inventories and greenhouse gas fluxes in coastal wetlands.

801 ~~Thanks~~Finally, ~~thanks~~ are extended to Chloe Bates for assisting with sample collection. ~~Finally,~~

802 we thank the editor and both reviewers for their comments which have improved this

803 manuscript.

804 **Reference List**

805 **References**

806 Ballantyne, C. K. and Small, D.: The Last Scottish Ice Sheet, Earth and Environmental Science

807 Transactions of The Royal Society of Edinburgh, 110, 93–131,

808 https://doi.org/10.1017/S1755691018000038, 2019.

809 Bao, R., Zhao, M., McNichol, A., Wu, Y., Guo, X., Haghipour, N., and Eglinton, T. I.: On the Origin

810 of Aged Sedimentary Organic Matter Along a River-Shelf-Deep Ocean Transect, Journal of

811 Geophysical Research: Biogeosciences, 124, 2582–2594,

812 https://doi.org/10.1029/2019JG005107, 2019.

Formatted: Plain Table 5

Formatted: Font: +Body (Aptos), 11 pt, Font color: Auto

Formatted: Heading 2, Left, Line spacing: single

Formatted: Left

Formatted: Font: (Default) +Body (Aptos), Font color: Auto

Formatted: Font: Not Bold

Formatted: Header

813 Bernal, B., Megonigal, J. P., and Mozdzer, T. J.: An invasive wetland grass primes deep soil carbon
814 pools, *Global Change Biology*, 23, 2104–2116, <https://doi.org/10.1111/gcb.13539>, 2017.

815 Boström, B., Comstedt, D., and Ekblad, A.: Isotope fractionation and ¹³C enrichment in soil
816 profiles during the decomposition of soil organic matter, *Oecologia*, 153, 89–98,
817 <https://doi.org/10.1007/s00442-007-0700-8>, 2007.

818 Brand, W. A., Coplen, T. B., Vogl, J., Rosner, M., and Prohaska, T.: Assessment of international
819 reference materials for isotope-ratio analysis (IUPAC Technical Report), *Pure and Applied*
820 *Chemistry*, 86, 425–467, <https://doi.org/10.1515/pac-2013-1023>, 2014.

821 Capel, E. L., de la Rosa Arranz, J. M., González-Vila, F. J., González-Perez, J. A., and Manning, D.
822 A. C.: Elucidation of different forms of organic carbon in marine sediments from the Atlantic
823 coast of Spain using thermal analysis coupled to isotope ratio and quadrupole mass
824 spectrometry, *Organic Geochemistry*, 37, 1983–1994,
825 <https://doi.org/10.1016/j.orggeochem.2006.07.025>, 2006.

826 Chapman, S. K., Hayes, M. A., Kelly, B., and Langley, J. A.: Exploring the oxygen sensitivity of
827 wetland soil carbon mineralization, *Biology Letters*, 15, 20180407,
828 <https://doi.org/10.1098/rsbl.2018.0407>, 2019.

829 Dasari, S., Garnett, M. H., and Hilton, R. G.: Leakage of old carbon dioxide from a major river
830 system in the Canadian Arctic, *PNAS Nexus*, 3, pgae134,
831 <https://doi.org/10.1093/pnasnexus/pgae134>, 2024.

832 Dean, J. F., Billett, M. F., Turner, T. E., Garnett, M. H., Andersen, R., McKenzie, R. M., Dinsmore, K.
833 J., Baird, A. J., Chapman, P. J., and Holden, J.: Peatland pools are tightly coupled to the
834 contemporary carbon cycle, *Global Change Biology*, n/a, e16999,
835 <https://doi.org/10.1111/gcb.16999>, 2023.

836 Etcheverría, P., Huygens, D., Godoy, R., Borie, F., and Boeckx, P.: Arbuscular mycorrhizal fungi
837 contribute to ¹³C and ¹⁵N enrichment of soil organic matter in forest soils, *Soil Biology and*
838 *Biochemistry*, 41, 858–861, <https://doi.org/10.1016/j.soilbio.2009.01.018>, 2009.

839 Garnett, M. H., Pereira, R., Taylor, C., Murray, C., and Ascough, P. L.: A NEW RAMPED
840 OXIDATION-¹⁴C ANALYSIS FACILITY AT THE NEIF RADIOCARBON LABORATORY, EAST KILBRIDE,
841 UK, *Radiocarbon*, 65, 1213–1229, <https://doi.org/10.1017/RDC.2023.96>, 2023.

Formatted: Plain Table 5

Formatted: Header

842 Granse, D., Wanner, A., Stock, M., Jensen, K., and Mueller, P.: Plant-sediment interactions
843 decouple inorganic from organic carbon stock development in salt marsh soils, *Limnology and*
844 *Oceanography Letters*, n/a, <https://doi.org/10.1002/lol2.10382>, 2024.

845 Hajdas, I., Ascough, P., Garnett, M. H., Fallon, S. J., Pearson, C. L., Quarta, G., Spalding, K. L.,
846 Yamaguchi, H., and Yoneda, M.: Radiocarbon dating, *Nat Rev Methods Primers*, 1, 1–26,
847 <https://doi.org/10.1038/s43586-021-00058-7>, 2021.

848 Hemingway, J. D., Galy, V. V., Gagnon, A. R., Grant, K. E., Rosengard, S. Z., Soulet, G., Zigah, P. K.,
849 and McNichol, A. P.: Assessing the Blank Carbon Contribution, Isotope Mass Balance, and
850 Kinetic Isotope Fractionation of the Ramped Pyrolysis/Oxidation Instrument at NOSAMS,
851 *Radiocarbon*, 59, 179–193, <https://doi.org/10.1017/RDC.2017.3>, 2017.

852 Houston, A., Garnett, M. H., and Austin, W. E. N.: Blue carbon additionality: New insights from
853 the radiocarbon content of saltmarsh soils and their respired CO₂, *Limnology and*
854 *Oceanography*, n/a, <https://doi.org/10.1002/lno.12508>, 2024.

855 Howard, J., Sutton-Grier, A. E., Smart, L. S., Lopes, C. C., Hamilton, J., Kleypas, J., Simpson, S.,
856 McGowan, J., Pessarrodona, A., Alleway, H. K., and Landis, E.: Blue carbon pathways for climate
857 mitigation: Known, emerging and unlikely, *Marine Policy*, 156, 105788,
858 <https://doi.org/10.1016/j.marpol.2023.105788>, 2023.

859 Komada, T., Bravo, A., Brinkmann, M.-T., Lu, K., Wong, L., and Shields, G.: “Slow” and “fast” in
860 blue carbon: Differential turnover of allochthonous and autochthonous organic matter in
861 minerogenic salt marsh sediments, *Limnology and Oceanography*, n/a,
862 <https://doi.org/10.1002/lno.12090>, 2022.

863 Leng, M. J. and Lewis, J. P.: C/N ratios and Carbon Isotope Composition of Organic Matter in
864 Estuarine Environments, in: *Applications of Paleoenvironmental Techniques in Estuarine*
865 *Studies*, edited by: Weckström, K., Saunders, K. M., Gell, P. A., and Skilbeck, C. G., Springer
866 Netherlands, Dordrecht, 213–237, https://doi.org/10.1007/978-94-024-0990-1_9, 2017.

867 Leng, M. J., Lamb, A. L., Heaton, T. H. E., Marshall, J. D., Wolfe, B. B., Jones, M. D., Holmes, J. A.,
868 and Arrowsmith, C.: Isotopes in Lake Sediments, in: *Isotopes in Palaeoenvironmental Research*,
869 edited by: Leng, M. J., Springer Netherlands, Dordrecht, 147–184, https://doi.org/10.1007/1-4020-2504-1_04, 2006.

Formatted: Plain Table 5

Formatted: Header

871 Leorri, E., Zimmerman, A. R., Mitra, S., Christian, R. R., Fatela, F., and Mallinson, D. J.: Refractory
872 organic matter in coastal salt marshes-effect on C sequestration calculations, Science of the
873 Total Environment, 633, 391–398, <https://doi.org/10.1016/j.scitotenv.2018.03.120>, 2018.

874 Luk, S. Y., Todd-Brown, K., Eagle, M., McNichol, A. P., Sanderman, J., Gosselin, K., and Spivak, A.
875 C.: Soil Organic Carbon Development and Turnover in Natural and Disturbed Salt Marsh
876 Environments, Geophysical Research Letters, 48, e2020GL090287,
877 <https://doi.org/10.1029/2020GL090287>, 2021.

878 Macreadie, P. I., Anton, A., Raven, J. A., Beaumont, N., Connolly, R. M., Friess, D. A., Kelleway, J.
879 J., Kennedy, H., Kuwae, T., Lavery, P. S., Lovelock, C. E., Smale, D. A., Apostolaki, E. T., Atwood, T.
880 B., Baldock, J., Bianchi, T. S., Chmura, G. L., Eyre, B. D., Fourqurean, J. W., Hall-Spencer, J. M.,
881 Huxham, M., Hendriks, I. E., Krause-Jensen, D., Laffoley, D., Luisetti, T., Marbà, N., Masque, P.,
882 McGlathery, K. J., Megonigal, J. P., Murdiyarso, D., Russell, B. D., Santos, R., Serrano, O.,
883 Silliman, B. R., Watanabe, K., and Duarte, C. M.: The future of Blue Carbon science, Nature
884 Communications, 10, 3998, <https://doi.org/10.1038/s41467-019-11693-w>, 2019.

885 Macreadie, P. I., Costa, M. D. P., Atwood, T. B., Friess, D. A., Kelleway, J. J., Kennedy, H.,
886 Lovelock, C. E., Serrano, O., and Duarte, C. M.: Blue carbon as a natural climate solution, Nat
887 Rev Earth Environ, 2, 826–839, <https://doi.org/10.1038/s43017-021-00224-1>, 2021.

888 McTigue, N. D., Walker, Q. A., and Currin, C. A.: Refining Estimates of Greenhouse Gas
889 Emissions From Salt Marsh “Blue Carbon” Erosion and Decomposition, Frontiers in Marine
890 Science, 8, 2021.

891 Miller, L. C., Smeaton, C., Yang, H., and Austin, W. E. N.: Carbon accumulation and storage
892 across contrasting saltmarshes of Scotland, Estuarine, Coastal and Shelf Science, 108223,
893 <https://doi.org/10.1016/j.ecss.2023.108223>, 2023.

894 Mueller, P., Do, H. T., Jensen, K., and Nolte, S.: Origin of organic carbon in the topsoil of Wadden
895 Sea salt marshes, Marine Ecology Progress Series, 624, 39–50,
896 <https://doi.org/10.3354/meps13009>, 2019.

897 Noyce, G. L., Smith, A. J., Kirwan, M. L., Rich, R. L., and Megonigal, J. P.: Oxygen priming induced
898 by elevated CO₂ reduces carbon accumulation and methane emissions in coastal wetlands,
899 Nat. Geosci., 16, 63–68, <https://doi.org/10.1038/s41561-022-01070-6>, 2023.

900 Peltre, C., Fernández, J. M., Craine, J. M., and Plante, A. F.: Relationships between Biological and
901 Thermal Indices of Soil Organic Matter Stability Differ with Soil Organic Carbon Level, Soil
902 Science Society of America Journal, 77, 2020–2028, <https://doi.org/10.2136/sssaj2013.02.0081>,
903 2013.

904 Plante, A. F., Fernández, J. M., and Leifeld, J.: Application of thermal analysis techniques in soil
905 science, Geoderma, 153, 1–10, <https://doi.org/10.1016/j.geoderma.2009.08.016>, 2009.

906 Plante, A. F., Fernández, J. M., Haddix, M. L., Steinweg, J. M., and Conant, R. T.: Biological,
907 chemical and thermal indices of soil organic matter stability in four grassland soils, Soil Biology
908 and Biochemistry, 43, 1051–1058, <https://doi.org/10.1016/j.soilbio.2011.01.024>, 2011.

909 Plante, A. F., Beaupré, S. R., Roberts, M. L., and Baisden, T.: Distribution of Radiocarbon Ages in
910 Soil Organic Matter by Thermal Fractionation, Radiocarbon, 55, 1077–1083,
911 <https://doi.org/10.1017/S0033822200058215>, 2013.

912 Ramnarine, R., Wagner-Riddle, C., Dunfield, K. E., and Voroney, R. P.: Contributions of
913 carbonates to soil CO₂ emissions, Can. J. Soil. Sci., 92, 599–607,
914 <https://doi.org/10.4141/cjss2011-025>, 2012.

915 Rumpel, C. and Kögel-Knabner, I.: Deep soil organic matter—a key but poorly understood
916 component of terrestrial C cycle, Plant Soil, 338, 143–158, [https://doi.org/10.1007/s11104-010-](https://doi.org/10.1007/s11104-010-0391-5)
917 0391-5, 2011.

918 Saintilan, N., Rogers, K., Mazumder, D., and Woodroffe, C.: Allochthonous and autochthonous
919 contributions to carbon accumulation and carbon store in southeastern Australian coastal
920 wetlands, Estuarine, Coastal and Shelf Science, 128, 84–92,
921 <https://doi.org/10.1016/j.ecss.2013.05.010>, 2013.

922 Sanderman, J. and Grandy, A. S.: Ramped thermal analysis for isolating biologically meaningful
923 soil organic matter fractions with distinct residence times, SOIL, 6, 131–144,
924 <https://doi.org/10.5194/soil-6-131-2020>, 2020.

925 Smeaton, C., Garrett, E., Koot, M. B., Ladd, C. J. T., Miller, L. C., McMahon, L., Foster, B., Barlow,
926 N. L. M., Blake, W., Gehrels, W. R., Skov, M. W., and Austin, W. E. N.: Organic carbon
927 accumulation in British saltmarshes, Science of The Total Environment, 926, 172104,
928 <https://doi.org/10.1016/j.scitotenv.2024.172104>, 2024.

Formatted: Plain Table 5

Formatted: Header

|

929 Soldatova, E., Krasilnikov, S., and Kuzyakov, Y.: Soil organic matter turnover: Global implications
930 from $\delta^{13}\text{C}$ and $\delta^{15}\text{N}$ signatures, *Science of The Total Environment*, 912, 169423,
931 <https://doi.org/10.1016/j.scitotenv.2023.169423>, 2024.

932 Stoner, S. W., Schrumpf, M., Hoyt, A., Sierra, C. A., Doetterl, S., Galy, V., and Trumbore, S.: How
933 well does ramped thermal oxidation quantify the age distribution of soil carbon? Assessing
934 thermal stability of physically and chemically fractionated soil organic matter, *Biogeosciences*,
935 20, 3151–3163, <https://doi.org/10.5194/bg-20-3151-2023>, 2023.

936 Van Dam, B. R., Zeller, M. A., Lopes, C., Smyth, A. R., Böttcher, M. E., Osburn, C. L., Zimmerman,
937 T., Prärfrock, D., Fourqurean, J. W., and Thomas, H.: Calcification-driven CO_2 emissions exceed
938 “Blue Carbon” sequestration in a carbonate seagrass meadow, *Science Advances*, 7, eabj1372,
939 <https://doi.org/10.1126/sciadv.abj1372>, 2021.

940 Van de Broek, M., Vandendriessche, C., Poppelmonde, D., Merckx, R., Temmerman, S., and
941 Govers, G.: Long-term organic carbon sequestration in tidal marsh sediments is dominated by
942 old-aged allochthonous inputs in a macrotidal estuary, *Global Change Biology*, 24, 2498–2512,
943 <https://doi.org/10.1111/gcb.14089>, 2018.

944 Werth, M. and Kuzyakov, Y.: ^{13}C fractionation at the root–microorganisms–soil interface: A
945 review and outlook for partitioning studies, *Soil Biology and Biochemistry*, 42, 1372–1384,
946 <https://doi.org/10.1016/j.soilbio.2010.04.009>, 2010.

947 Williams, E. K. and Plante, A. F.: A Bioenergetic Framework for Assessing Soil Organic Matter
948 Persistence, *Frontiers in Earth Science*, 6, 2018.

949
950
951
952
953
954
955
956

Formatted: Plain Table 5

Formatted: Header

|

957
958
959
960
961
962
963
964
965

Formatted: Plain Table 5

Formatted: Font: Not Bold

|

Formatted: Header